



Controllability of the linear 1D-wave equation with inner moving forces

Castro Carlos, Nicolae Cindea, Arnaud Munch

► To cite this version:

Castro Carlos, Nicolae Cindea, Arnaud Munch. Controllability of the linear 1D-wave equation with inner moving forces. *SIAM Journal on Control and Optimization*, 2014, 52 (6), pp. 4027-4056. 10.1137/140956129 . hal-00927076v2

HAL Id: hal-00927076

<https://hal.science/hal-00927076v2>

Submitted on 20 Jan 2014

HAL is a multi-disciplinary open access archive for the deposit and dissemination of scientific research documents, whether they are published or not. The documents may come from teaching and research institutions in France or abroad, or from public or private research centers.

L'archive ouverte pluridisciplinaire **HAL**, est destinée au dépôt et à la diffusion de documents scientifiques de niveau recherche, publiés ou non, émanant des établissements d'enseignement et de recherche français ou étrangers, des laboratoires publics ou privés.

Controllability of the linear 1D wave equation with inner moving forces

CARLOS CASTRO*

NICOLAE CÎNDEA†

ARNAUD MÜNCH†

January 20, 2014

Abstract

This paper deals with the numerical computation of distributed null controls for the 1D wave equation. We consider supports of the controls that may vary with respect to the time variable. The goal is to compute approximations of such controls that drive the solution from a prescribed initial state to zero at a large enough controllability time. Assuming a geometric optic condition on the support of the controls, we first prove a generalized observability inequality for the homogeneous wave equation. We then introduce and prove the well-posedness of a mixed formulation that characterizes the controls of minimal square-integrable norm. Such mixed formulation, introduced in [Cindea and Münch, *A mixed formulation for the direct approximation of the control of minimal L^2 -norm for linear type wave equations*], and solved in the framework of the (space-time) finite element method, is particularly well-adapted to address the case of time dependent support. Several numerical experiments are discussed.

Keywords: Linear wave equation, null controllability, finite element methods, Mixed formulation.

Mathematics Subject Classification (2010)- 35L10, 65M12, 93B40.

1 Introduction

Let T be a positive real, Q_T the domain $(0, 1) \times (0, T)$, q_T a non-empty subset of Q_T and $\Sigma_T = \{0, 1\} \times (0, T)$. We are concerned in this work with the null distributed controllability for the 1D wave equation:

$$\begin{cases} y_{tt} - y_{xx} = v \mathbf{1}_{q_T}, & (x, t) \in Q_T \\ y(x, t) = 0, & (x, t) \in \Sigma_T \\ y(x, 0) = y_0(x), \quad y_t(x, 0) = y_1(x), & x \in (0, 1). \end{cases} \quad (1)$$

We assume that $(y_0, y_1) \in \mathbf{V} := H_0^1(0, 1) \times L^2(0, 1)$; $v = v(t)$ is the *control* (a function in $L^2(q_T)$) and $y = y(x, t)$ is the associated state. $\mathbf{1}_{q_T}$ from Q_T to $\{0, 1\}$ denotes the indicatrice function of q_T . We also use the notation:

$$L y := y_{tt} - y_{xx}. \quad (2)$$

For any $(y_0, y_1) \in \mathbf{V}$ and any $v \in L^2(q_T)$, there exists exactly one solution y to (1), with the regularity $y \in C^0([0, T]; H_0^1(0, 1)) \cap C^1([0, T]; L^2(0, 1))$ (see [19]).

*Dep. Matematica e Informatica, ETSI Caminos, Canales y Puertos, Universidad Politecnica de Madrid, 28040 Madrid, Spain. E-mail: carlos.castro@upm.es.

†Laboratoire de Mathématiques, Université Blaise Pascal (Clermont-Ferand 2), UMR CNRS 6620, Campus de Cézeaux, 63177, Aubière, France. E-mails: nicolae.cindea@math.univ-bpclermont.fr, arnaud.munch@math.univ-bpclermont.fr.

The null controllability problem for (1) at time T is the following: for each $(y_0, y_1) \in \mathbf{V}$, find $v \in L^2(q_T)$ such that the corresponding solution to (1) satisfies

$$y(\cdot, T) = 0, \quad y_t(\cdot, T) = 0 \quad \text{in } (0, 1). \quad (3)$$

When the subset q_T takes the form $q_T := \omega \times (0, T)$, where ω denotes a subset of $(0, 1)$, the null-controllability of (1) at any *large* time $T > T^*$ is well-known (for instance, see [1, 19]). The critical time T^* is related to the measure of $(0, 1) \setminus \omega$. Moreover, as a consequence of the *Hilbert Uniqueness Method* of J.-L. Lions [19], the null controllability of (1) is equivalent to an observability inequality for the associated adjoint problem : there exists $C > 0$ such that

$$\|\varphi(\cdot, 0), \varphi_t(\cdot, 0)\|_{\mathbf{H}}^2 \leq C \|\varphi\|_{L^2(\omega \times (0, T))}^2, \quad \forall (\varphi_0, \varphi_1) \in \mathbf{H} := L^2(0, 1) \times H^{-1}(0, 1) \quad (4)$$

where $(\varphi, \varphi_0, \varphi_1)$ solves

$$L\varphi = 0 \quad \text{in } Q_T, \quad \varphi = 0 \quad \text{on } \Sigma_T; \quad (\varphi(\cdot, 0), \varphi_t(\cdot, 0)) = (\varphi_0, \varphi_1) \quad \text{in } (0, 1). \quad (5)$$

We investigate in this work some questions related to the controllability of (1) for more general subsets $q_T \subset Q_T$ where the support of the control function v depends on the time variable. A particular example is to consider the region between two curves, i.e.

$$q_T = \left\{ (x, t) \in Q_T; a(t) < x < b(t), t \in (0, T) \right\}. \quad (6)$$

A geometrical description is given by Figure 1.

To our knowledge, the control of PDEs with non-cylindrical support has been much less addressed in the literature. For the wave equation, we mention the contribution of Khapalov [18] providing observability results for a moving point sensor in the interior of the domain, allowing the author to avoid the usual difficulties related to strategic or non-strategic points. In particular, in the 1D setting, for any $T > 0$, the existence of controls continuous almost everywhere in $(0, T)$, supported over curves continuous almost everywhere is obtained for data in $H^2(0, 1) \cap H_0^1(0, 1) \times H_0^1(0, 1)$. More recently, let us mention two works concerning again the 1D wave equation both for initial data in \mathbf{H} and any $T > 2$: the first one [6] analyzes the exact controllability from a moving interior point. By the way of the d'Alembert formula, an observability inequality is proved for a precise sets of curves $\{(\gamma(t), t)\}_{t \in (0, T)}$ leading to moving controls in $H^{-1}(\cup_{t \in (0, T)} \gamma(t) \times \{t\})$. The second one [11] considers the controllability from the moving boundary of the form $1 + kt$ with $k \in (0, 1]$, $t \in (0, T)$. In the case $k < 1$, the controllability in $L^2(0, T)$ is proved by the way of the multiplier method: as is usual, a change of variable reduces the problem on fixed domains for wave equation with non constants coefficient. In the case $k = 1$ for which the speed of the moving endpoint is equal to the characteristic speed, the d'Alembert formula allows to characterize the reachable set. Eventually, we mention that in [20], the authors prove that a mobile control support in time allows to recover the controllability of the damped wave equation $y_{tt} - y_{xx} - \varepsilon y_{txx} = 0$ defined on the 1D torus, uniformly with respect to the parameter $\varepsilon > 0$ (due the appearance of an essential spectrum as $\varepsilon \rightarrow 0$, the uniform controllability property can not be obtained if the control simply acts on a cylindrical domain).

Let us denote by $\mathcal{C}(a, b, T)$ the class of domains of the form given by (6) for which the controllability holds, or equivalently the set of triplet $(a, b, T) \in C([0, T],]0, 1[) \times C([0, T],]0, 1[) \times \mathbf{R}^+$ for which the controllability hold. Obviously, this set is not empty: it suffices that T be large enough and that the domain $\{(x, t) \in Q_T; a(t) < x < b(t), t \in (0, T)\}$ contains any rectangular domain $(a_1, b_1) \times (0, T)$ (i.e. that there exists $a_1 > 0, b_1 > 0$ such that $a(t) \leq a_1 < b_1 \leq b(t)$ for all time $t \in [0, T]$) and then to apply (4).

The first contribution of this work is the extension of the well-known observability inequality (4) to time-depending subsets q_T , as for instance those given by (6). Precisely, we prove that if

$T > 2$ and any characteristic line starting at any point $x \in (0, 1)$ at time $t = 0$ and following the optical geometric conditions when reflecting at the boundary $x = 0, 1$, meets the observation subset q_T then the following estimate turns out to be true :

$$\|\varphi(\cdot, 0), \varphi_t(\cdot, 0)\|_{\mathbf{H}}^2 \leq C \left(\|\varphi\|_{L^2(q_T)}^2 + \|L\varphi\|_{L^2(0, T; H^{-1}(0, 1))}^2 \right), \quad \forall \varphi \in \Phi \quad (7)$$

where $\Phi = \{\varphi : \varphi \in L^2(q_T), \varphi = 0 \text{ on } \Sigma_T \text{ such that } L\varphi \in L^2(0, T; H^{-1}(0, 1))\}$. This so-called generalized inequality observability implies by duality arguments the null controllability of (1) with controls in $L^2(q_T)$ for q_T given by (6).

The second contribution of this work is the introduction of a numerical method for the approximation of the control of minimal $L^2(q_T)$ -norm. Usually (for instance see [16, 17, 22]), such approximation is based on the minimization of the so-called conjugate functional :

$$\min_{(\varphi_0, \varphi_1) \in \mathbf{H}} J^*(\varphi_0, \varphi_1) = \frac{1}{2} \iint_{q_T} |\varphi|^2 dx dt + \langle \varphi_1, y_0 \rangle_{H^{-1}(0, 1), H_0^1(0, 1)} - \int_0^1 \varphi_0 y_1 dx \quad (8)$$

where $(\varphi, \varphi_0, \varphi_1)$ solves (5). Here and in the sequel, we use the following duality pairing :

$$\langle \varphi_1, y_0 \rangle_{H^{-1}(0, 1), H_0^1(0, 1)} = \int_0^1 \partial_x ((-\Delta)^{-1} \varphi_1)(x) \partial_x y_0(x) dx$$

where $-\Delta$ is the Dirichlet Laplacian in $(0, 1)$. The well-posedness of this extremal problem - precisely the coercivity of J^* over \mathbf{H} - is given by the estimate (7). The control of minimal $L^2(q_T)$ -norm is then given by $v = -\varphi 1_{q_T}$ where φ solves (5) associated to (φ_0, φ_1) , unique minimizer of J^* . Since the domain q_T evolves in time, the resolution of the wave equation by any usual time marching method leads to some technicalities (at the level of the numerical implementation). We therefore use, in the spirit of the works [9, 10], an equivalent formulation where the time and the space variables are embedded in a time-space variational formulation, very appropriate to our non-cylindrical situation. Specifically, we consider the following extremal problem over the variable φ :

$$\min_{\varphi \in W} \hat{J}^*(\varphi) = \frac{1}{2} \iint_{q_T} |\varphi|^2 dx dt + \langle \varphi_1, y_0 \rangle_{H^{-1}(0, 1), H_0^1(0, 1)} - \int_0^1 \varphi_0 y_1 dx, \quad (9)$$

with $W = \{\varphi : \varphi \in L^2(q_T), \varphi = 0 \text{ on } \Sigma_T \text{ such that } L\varphi = 0 \in L^2(0, T; H^{-1}(0, 1))\}$. The unknown is now the whole solution φ , constrained by the equality $L\varphi = 0$ in $L^2(0, T; H^{-1}(0, 1))$. This constraint is taken into account with a Lagrangian multiplier $\lambda \in L^2(0, T; H_0^1(0, 1))$ through a mixed formulation in (φ, λ) solved using a conformal finite element approximation in time and space.

This paper is organized as follows. In Section 2, we prove the generalized observability inequality (7) over the Hilbert space Φ (see Proposition 2.1) leading to the uniform controllability of (1) in \mathbf{V} . In Section 3, we adapt [10] and introduce the mixed formulation (24) in the variable $(\varphi, \lambda) \in \Phi \times L^2(0, T; H_0^1(0, 1))$ equivalent to the extremal problem (9). The variable λ can be interpreted as a Lagrange multiplier for the equality constraint $L\varphi = 0$ in $L^2(0, T; H^{-1}(0, 1))$. We employ the estimate (7) to prove the well-posedness of this mixed formulation. In particular, we prove an inf-sup condition for the pair (φ, λ) . Moreover, it turns out that the multiplier λ , unique solution of the mixed formulation, coincides with the controlled state y , solution of (1) (in the weak-sense) (see section 3.1). This property allows to define Section 3.2 an another equivalent extremal problem (the so-called primal problem, dual of the problem (9)) in the controlled solution y only (see Proposition 3.1), without the introduction of any penalty parameter. The corresponding elliptic problem in $L^2(0, T; H_0^1(0, 1))$ is solved by the way of a conjugate gradient algorithm. Section 4 is devoted to the numerical approximation of the mixed formulation as well as some numerical experiments. We emphasize the robustness of the approach leading notably to the strong convergence of discrete

sequence $\{v_h\}$ toward the controls for various geometries of q_T . Eventually, Section 5 concludes with some perspectives: in particular, we highlight the natural extension of this work which consists in optimizing the control of (1) with respect to the support q_T .

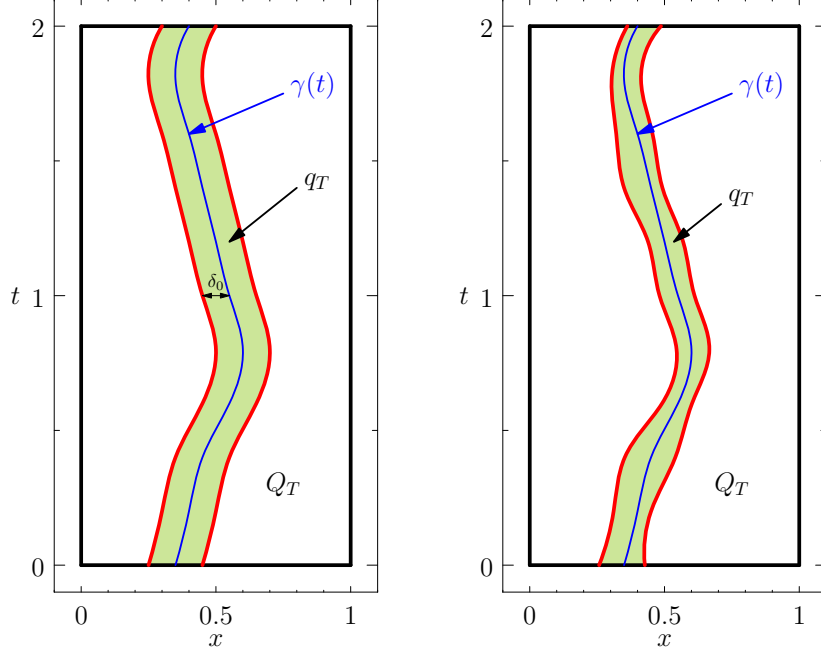


Figure 1: Time dependent domains q_T included in Q_T .

2 A generalized observability inequality

Let $q_T \subset (0, 1) \times (0, T)$ be an open set. We define the vectorial space

$$\Phi = \left\{ \varphi : \varphi \in L^2(q_T), \varphi = 0 \text{ on } \Sigma_T \text{ such that } L\varphi \in L^2(0, T; H^{-1}(0, 1)) \right\}.$$

Endowed with the following inner product

$$(\varphi, \bar{\varphi})_\Phi = \iint_{q_T} \varphi(x, t) \bar{\varphi}(x, t) dx dt + \eta \int_0^T \langle L\varphi, L\bar{\varphi} \rangle_{H^{-1}(0, 1), H^{-1}(0, 1)} dt, \quad (10)$$

for any fixed $\eta > 0$, the space Φ is an Hilbert space.

In this section, we prove the following result.

PROPOSITION 2.1 *Assume that $T > 2$ and $q_T \subset (0, 1) \times (0, T)$ is a finite union of connected open sets and satisfies the following hypotheses: Any characteristic line starting at the point $x \in (0, 1)$ at time $t = 0$ and following the optical geometric laws when reflecting at the boundaries $x = 0, 1$ must meet q_T .*

Then, there exists $C > 0$ such that the following estimate holds :

$$\|\varphi(\cdot, 0), \varphi_t(\cdot, 0)\|_{\mathbf{H}}^2 \leq C \left(\|\varphi\|_{L^2(q_T)}^2 + \|L\varphi\|_{L^2(0, T; H^{-1}(0, 1))}^2 \right), \quad \forall \varphi \in \Phi. \quad (11)$$

PROOF: We proceed in several steps:

Step 1: Let φ be a smooth solutions of the wave equation (5). Note that φ can be extended in a unique way to a function, still denoted by φ , in $(x, t) \in (0, 1) \times \mathbf{R}$ satisfying $L\varphi = 0$ and the boundary conditions $\varphi(0, t) = \varphi(1, t) = 0$ for all $t \in \mathbf{R}$. In this first step we prove that for such extension the following holds: For each $t \in \mathbf{R}$, $x \in (0, 1)$ and $\delta > 0$

$$\int_{t-\delta}^{t+\delta} \varphi_x(0, s) ds \leq \frac{1}{\delta} \iint_{\mathcal{U}_{(x, t+x)}^\delta} (|\varphi_x(y, s)|^2 + |\varphi_t(y, s)|^2) dy ds, \quad (12)$$

$$\int_{t-\delta}^{t+\delta} \varphi_x(0, s) ds \leq \frac{1}{\delta} \iint_{\mathcal{U}_{(x, t-x)}^\delta} (|\varphi_x(y, s)|^2 + |\varphi_t(y, s)|^2) dy ds, \quad (13)$$

where $\mathcal{U}_{(x, t)}^\delta$ is a neighborhood of (x, t) of the form $\mathcal{U}_{(x, t)}^\delta = \{(y, s) \text{ such that } |x - y| + |t - s| < \delta\}$.

Let us start with (12). Note that wave equation is symmetric with respect to the time and space variables. Therefore, the D'Alembert formulae can be used changing the time and space role, i.e.

$$\frac{1}{2} \int_{t-x}^{t+x} u_x(0, s) ds = u(x, t), \quad (x, t) \in (0, 1) \times \mathbf{R}, \quad (14)$$

where we have taken into account the boundary condition $u(0, t) = 0$. Consider now $x = x_0 - t$ in (14) and differentiate with respect to time. Then,

$$-\varphi_x(0, 2t - x_0) = -\varphi_x(x_0 - t, t) + \varphi_t(x_0 - t, t),$$

that written in the original variables (x, t) gives,

$$\varphi_x(0, t - x) = \varphi_x(x, t) - \varphi_t(x, t),$$

or equivalently

$$\varphi_x(0, t) = \varphi_x(x, t + x) - \varphi_t(x, t + x), \quad t \in \mathbf{R}, \quad x \in (0, 1). \quad (15)$$

Integrating the square of (15) in $(y, s) \in \mathcal{U}_{(x, t+x)}^\delta$ with the parametrization

$$\begin{cases} y = x + \frac{u-v}{\sqrt{2}} \\ s = t + x + \frac{u+v}{\sqrt{2}} \end{cases}, \quad |u|, |v| < \delta/\sqrt{2},$$

we obtain

$$\int_{-\delta/\sqrt{2}}^{\delta/\sqrt{2}} \int_{-\delta/\sqrt{2}}^{\delta/\sqrt{2}} |u_x(0, t + 2v/\sqrt{2})|^2 du dv = \iint_{\mathcal{U}_{(x, t+x)}^\delta} |u_x(y, s) - u_t(y, s)|^2 dy ds.$$

Therefore, with the change $s = t + 2v/\sqrt{2}$ in the first integral, we easily obtain (12). Formula (13) is obtained in a similar way but this time with the change $x = x_0 + t$ in (14).

Step 2. Here we show that there exists a constant $C > 0$ such that,

$$\|\varphi(\cdot, 0), \varphi_t(\cdot, 0)\|_{\mathbf{V}}^2 \leq C \left(\|\varphi_t\|_{L^2(q_T)}^2 + \|\varphi_x\|_{L^2(q_T)}^2 \right), \quad (16)$$

for any $\varphi \in W$ and initial data in \mathbf{V} .

We may assume that φ is smooth since the general case can be obtained by a usual density argument. We also assume that φ is extended to $(x, t) \in (0, 1) \times \mathbf{R}$ by assuming that it satisfies the wave equation and boundary conditions in this region. This extension is unique and 2-periodic in time. The region q_T is also extended to \tilde{q}_T to take advantage of the time periodicity of the solution φ . We define,

$$\tilde{q}_T = \bigcup_{k \in \mathbb{Z}} \{(x, t) \text{ such that } (x, t + 2k) \in q_T\}.$$

The key point now is to observe that the hypotheses on q_T , namely the fact that any characteristic line starting at point $(x, 0)$ and following the optical geometric laws when reflecting at the boundary must meet q_T , is equivalent to the following: For any point $(0, t)$ with $t \in [0, T]$ there exists one characteristic line (either $(x, t+x)$ with $x \in (0, 1)$ or $(x, t-x)$) that meets \tilde{q}_T .

Thus, given $t \in [0, T]$ we can apply either (12) with $(x, t+x) \in \tilde{q}_T$ or (13) with $(x, t-x) \in \tilde{q}_T$. Moreover, as \tilde{q}_T is an open set, we may assume δ sufficiently small so that the neighborhoods $\mathcal{U}_{(x, t+x)}^\delta \subset \tilde{q}_T$ or $\mathcal{U}_{(x, t-x)}^\delta \subset \tilde{q}_T$. In particular we see that for any $t \in [0, T]$ there exists $\delta_t > 0$ and $C_t > 0$ such that

$$\int_{t-\delta_t}^{t+\delta_t} |\varphi_x(0, s)|^2 ds \leq C_t \iint_{\tilde{q}_T} (|\varphi_t|^2 + |\varphi_x|^2) dx dt.$$

By compactity, there exists a finite number of times t_1, \dots, t_n such that $\cup_{i=1, \dots, n} (t_i - \delta_{t_i}, t_i + \delta_{t_i})$ covers the whole interval $[0, T]$ and therefore, by adding the corresponding inequalities, there exists $C > 0$ such that

$$\int_0^T |\varphi_x(0, s)|^2 ds \leq C \iint_{\tilde{q}_T} (|\varphi_t|^2 + |\varphi_x|^2) dx dt. \quad (17)$$

The fact that we can replace \tilde{q}_T by q_T is easily checked by the 2-periodicity of φ in time. Finally, it remains to see that we can replace the left hand side in (17) by $\|\varphi(\cdot, 0), \varphi_t(\cdot, 0)\|_{\mathbf{V}}^2$, but this is a consequence of the well-known boundary observability inequality (see for instance [19])

$$\|\varphi(\cdot, 0), \varphi_t(\cdot, 0)\|_{\mathbf{V}}^2 \leq C \int_0^T |\varphi_x(0, s)|^2 ds$$

which holds for $T > 2$.

Step 3. Here we show that we can substitute φ_x by φ in the right hand side of (16), i.e.

$$\|\varphi(\cdot, 0), \varphi_t(\cdot, 0)\|_{\mathbf{V}}^2 \leq C \left(\|\varphi_t\|_{L^2(q_T)}^2 + \|\varphi\|_{L^2(q_T)}^2 \right), \quad (18)$$

for any $\varphi \in W$ and initial data in \mathbf{V} . In fact, this requires to extend slightly the observation zone q_T . Instead, we observe that if q_T satisfies the hypotheses in Proposition 2.1 then there exists a smaller open subset $\tilde{q}_T \subset q_T$ that still satisfies the same hypotheses and such that the closure of \tilde{q}_T is included in q_T . Thus, (16) must hold as well for \tilde{q}_T . Let us introduce now a function $\eta \geq 0$ which satisfies the following hypotheses:

$$\eta \in C^1((0, 1) \times (0, T)), \quad \text{supp}(\eta) \subset q_T, \quad \|\eta_t\|_{L^\infty} + \|\eta_x^2/\eta\|_{L^\infty} \leq C_1 \quad \text{in } q_T$$

$$\eta > \eta_0 > 0 \quad \text{in } \tilde{q}_T, \quad \text{with } \eta_0 > 0 \text{ constant.}$$

As q_T is a finite union of connected open sets, the function η can be easily obtained by convolution of the characteristic function of \tilde{q}_T with a positive mollifier.

Multiplying the equation of φ by $\eta\varphi$ and integrating by parts we easily obtain

$$\begin{aligned} \iint_{q_T} \eta |\varphi_x|^2 dx dt &= \iint_{q_T} \eta |\varphi_t|^2 dx dt + \iint_{q_T} (\eta_t \varphi \varphi_t - \eta_x \varphi \varphi_x) dx dt \\ &\leq \iint_{q_T} \eta |\varphi_t|^2 dx dt + \frac{\|\eta_t\|_{L^\infty(q_T)}}{2} \iint_{q_T} (|\varphi|^2 + |\varphi_t|^2) dx dt \\ &\quad + \frac{1}{2} \iint_{q_T} \left(\frac{\eta_x^2}{\eta} \varphi^2 + \eta \varphi_x^2 \right) dx dt. \end{aligned}$$

Therefore,

$$\iint_{q_T} \eta |\varphi_x|^2 dx dt \leq C \iint_{q_T} (|\varphi_t|^2 + |\varphi|^2) dx dt,$$

for some constant $C > 0$, and we obtain

$$\|\varphi_x\|_{L^2(\tilde{q}_T)}^2 \leq C_2^{-1} \iint_{q_T} \eta |\varphi_x|^2 dx dt \leq C_2^{-1} C \iint_{q_T} (|\varphi_t|^2 + |\varphi|^2) dx dt.$$

This combined with (16) for \tilde{q}_T provides (18).

Step 4. Here we prove that we can remove the second term in the right hand side of (18), i.e.

$$\|\varphi(\cdot, 0), \varphi_t(\cdot, 0)\|_{\mathbf{V}}^2 \leq C \|\varphi_t\|_{L^2(q_T)}^2, \quad (19)$$

for any $\varphi \in W$ and initial data in \mathbf{V} . Note that, for each time $t \in [0, T]$ and each $\omega \subset \Omega$ we have the following regularity estimate

$$\int_{a(t)}^{b(t)} |\varphi(x, t)|^2 dx \leq \|\varphi(\cdot, 0), \varphi_t(\cdot, 0)\|_{\mathbf{H}}^2, \quad \text{for all } t \in [0, T]$$

Therefore, integrating in time, we easily obtain

$$\|\varphi\|_{L^2(q_T)}^2 \leq T \|\varphi(\cdot, 0), \varphi_t(\cdot, 0)\|_{\mathbf{H}}^2.$$

We now substitute this inequality in (16)

$$\|\varphi(\cdot, 0), \varphi_t(\cdot, 0)\|_{\mathbf{V}}^2 \leq C \left(\|\varphi_t\|_{L^2(q_T)}^2 + \|\varphi(\cdot, 0), \varphi_t(\cdot, 0)\|_{\mathbf{H}}^2 \right). \quad (20)$$

Inequality (19) is finally obtained by contradiction. Assume that it is not true. Then, there exists a sequence $(\varphi^k(\cdot, 0), \varphi_t^k(\cdot, 0))_{k>0} \in \mathbf{V}$ such that

$$\begin{aligned} \|\varphi^k(\cdot, 0), \varphi_t^k(\cdot, 0)\|_{\mathbf{V}}^2 &= 1, \quad \forall k > 0 \\ \|\varphi_t^k\|_{L^2(q_T)}^2 &\rightarrow 0, \quad \text{as } k \rightarrow \infty. \end{aligned}$$

Therefore, there exists a subsequence, still denoted by the index k , such that $(\varphi^k(\cdot, 0), \varphi_t^k(\cdot, 0)) \rightarrow (\varphi^*(\cdot, 0), \varphi_t^*(\cdot, 0))$ weakly in \mathbf{V} and strongly in \mathbf{H} (by the compactness of the inclusion $\mathbf{V} \subset \mathbf{H}$). Passing to the limit in the equation we easily see that the solution associated to $(\varphi^*(\cdot, 0), \varphi_t^*(\cdot, 0))$, φ^* must vanish at q_T and therefore, by (18), $\varphi^* = 0$. In particular this is in contradiction with (20) since it implies that the right hand side in (20) vanishes as $k \rightarrow \infty$ while the left hand side is bounded by below.

Step 5. We now write (19) with respect to the weaker norm. In particular, we obtain

$$\|\varphi(\cdot, 0), \varphi_t(\cdot, 0)\|_{\mathbf{H}}^2 \leq C \|\varphi\|_{L^2(q_T)}^2, \quad (21)$$

for any $\varphi \in \Phi$ with $L\varphi = 0$.

Let $\eta \in \Phi$ be the solution of $L\eta = 0$ and initial data $(\Delta^{-1}\varphi_t(\cdot, 0), \varphi(\cdot, 0)) \in \mathbf{V}$ where Δ designates the Dirichlet Laplacian in $(0, 1)$. Let us write $\eta(x, t) = \eta(x, 0) + \int_0^t \varphi(x, s) ds$, for all $(x, t) \in Q_T$. Then, inequality (19) on η and the fact that Δ is an isomorphism from $H_0^1(0, 1)$ to $H^{-1}(0, 1)$, provide

$$\begin{aligned} \|(\varphi(\cdot, 0), \varphi_t(\cdot, 0))\|_{\mathbf{H}}^2 &= \|(\Delta^{-1}\varphi_t(\cdot, 0), \varphi(\cdot, 0))\|_{\mathbf{V}}^2 \\ &\leq C \|\eta_t\|_{L^2(q_T)}^2 = C \|\varphi\|_{L^2(q_T)}^2. \end{aligned}$$

Step 6. Here we finally obtain (11). Given $\varphi \in \Phi$ we can decompose it as $\varphi = \varphi_1 + \varphi_2$ where $\varphi_1, \varphi_2 \in \Phi$ solve

$$\begin{cases} L\varphi_1 = L\varphi, \\ \varphi_1(\cdot, 0) = (\varphi_1)_t(\cdot, 0) = 0 \end{cases} \quad \begin{cases} L\varphi_2 = 0, \\ \varphi_2(\cdot, 0) = \varphi(\cdot, 0), \quad (\varphi_2)_t(\cdot, 0) = \varphi_t(\cdot, 0). \end{cases}$$

From Duhamel's principle, we can write

$$\varphi_1(\cdot, t) = \int_0^t \psi(\cdot, t-s, s) ds$$

where $\psi(x, t, s)$ solves, for each value of the parameter $s \in (0, t)$,

$$\begin{cases} L\psi(\cdot, \cdot, s) = 0, \\ \psi(\cdot, 0, s) = 0, \quad \psi_t(\cdot, 0, s) = L\varphi(\cdot, s). \end{cases}$$

Therefore,

$$\begin{aligned} \|\varphi_1\|_{L^2(q_T)}^2 &\leq \int_0^T \|\psi(\cdot, \cdot, s)\|_{L^2(q_T)}^2 ds \leq C \int_0^T \|\psi(\cdot, 0, s), \psi_t(\cdot, 0, s)\|_{\mathbf{H}}^2 ds \\ &\leq C \|L\varphi\|_{L^2(0,T;H^{-1}(0,1))}^2 \end{aligned} \quad (22)$$

Combining (22) and estimate (21) for φ_2 we obtain

$$\begin{aligned} \|\varphi(\cdot, 0), \varphi_t(\cdot, 0)\|_{\mathbf{H}}^2 &= \|\varphi_2(\cdot, 0), (\varphi_2)_t(\cdot, 0)\|_{\mathbf{H}}^2 \leq C \|\varphi_2\|_{L^2(q_T)}^2 \\ &\leq C \left(\|\varphi\|_{L^2(q_T)}^2 + \|\varphi_1\|_{L^2(q_T)}^2 \right) \leq C \left(\|\varphi\|_{L^2(q_T)}^2 + \|L\varphi\|_{L^2(0,T;H^{-1})}^2 \right). \end{aligned}$$

□

Remark 1 1. The hypotheses on q_T stated in Proposition 2.1 are optimal in the following sense: If there exists a subinterval $\omega_0 \subset (0, 1)$ for which all characteristics starting in ω_0 and following the geometrical optics conditions when getting to the boundary $x = 0, 1$, do not meet q_T , then the inequality fails to hold. This is easily seen by considering particular solutions of the wave equation which initial data supported in ω_0 .

2. The proof of inequality (11) above does not provide an estimate on the dependence of the constant with respect to q_T .

3. In the cylindrical situation, i.e. $q_T = (a, b) \times (0, T)$, a generalized Carleman inequality, valid for the wave equation with variable coefficients, have been obtained in [9] (see also [26]). To our knowledge, the extension of Proposition 2.1 to the wave equation with variable coefficients is still open and a priori can not be obtained by the method used in this section.

3 Control of minimal $L^2(q_T)$ -norm: a mixed reformulation

We now adapt in this section the work [10] and present a mixed formulation based on the optimality conditions associated to the extremal problem (8) (section 3.1). From a numerical point of view, this mixed formulation is more appropriate to the non-cylindrical situation considered in this work.

3.1 Mixed reformulation of the controllability problem

As described at length in [10], the starting point of the reformulation is the dual problem (8). Thus, in order to avoid the minimization of the functional J^* with respect to the initial data (φ_0, φ_1) , we now present a direct way to approximate the control of minimal square integrable norm, in the spirit of the primal approach developed in [9]. Since the variable φ , solution of (5), is completely and uniquely determined by the data (φ_0, φ_1) , the main idea of the reformulation is to keep φ as main variable and consider the following extremal problem:

$$\min_{\varphi \in W} \hat{J}^*(\varphi) = \frac{1}{2} \iint_{q_T} |\varphi|^2 dx dt + \langle \varphi_t(\cdot, 0), y_0 \rangle_{H^{-1}(0,1), H_0^1(0,1)} - \int_0^1 \varphi(\cdot, 0) y_1 dx, \quad (23)$$

where

$$W = \{ \varphi : \varphi \in L^2(Q_T), \varphi = 0 \text{ on } \Sigma_T \text{ such that } L\varphi = 0 \},$$

endowed with the same inner product than Φ , given in (10).

Remark that from (11) the property $\varphi \in W$ implies that $(\varphi(\cdot, 0), \varphi_t(\cdot, 0)) \in \mathbf{H}$, so that the functional \hat{J}^* is well-defined over W . Therefore, the minimization of \hat{J}^* is evidently equivalent to the minimization of J^* over \mathbf{H} .

The main variable is now φ submitted to the constraint equality $L\varphi = 0$ as an $L^2(0, T; H^{-1}(0, 1))$ function. This constraint is addressed introducing a Lagrangian multiplier $\lambda \in L^2(0, T; H_0^1(\Omega))$ as follows:

We consider the following problem : find $(\varphi, \lambda) \in \Phi \times L^2(0, T; H_0^1(0, 1))$ solution of

$$\begin{cases} a(\varphi, \bar{\varphi}) + b(\bar{\varphi}, \lambda) = l(\bar{\varphi}), & \forall \bar{\varphi} \in \Phi \\ b(\varphi, \bar{\lambda}) = 0, & \forall \bar{\lambda} \in L^2(0, T; H_0^1(0, 1)), \end{cases} \quad (24)$$

where

$$\begin{aligned} a : \Phi \times \Phi &\rightarrow \mathbb{R}, \quad a(\varphi, \bar{\varphi}) = \iint_{Q_T} \varphi \bar{\varphi} dx dt \\ b : \Phi \times L^2(0, T; H_0^1(0, 1)) &\rightarrow \mathbb{R}, \quad b(\varphi, \lambda) = \int_0^T \langle L\varphi, \lambda \rangle_{H^{-1}(0,1), H_0^1(0,1)} dt \\ &= \iint_{Q_T} \partial_x(-\Delta^{-1}(L\varphi)) \cdot \partial_x \lambda dx dt \\ l : \Phi &\rightarrow \mathbb{R}, \quad l(\varphi) = - \langle \varphi_t(\cdot, 0), y_0 \rangle_{H^{-1}(0,1), H_0^1(0,1)} + \int_0^1 \varphi(\cdot, 0) y_1 dx. \end{aligned}$$

We have the following result :

THEOREM 3.1 *Under the hypothesis of Proposition 2.1, we have :*

- (i) *The mixed formulation (24) is well-posed.*
- (ii) *The unique solution $(\varphi, \lambda) \in \Phi \times L^2(0, T; H_0^1(0, 1))$ is the unique saddle-point of the Lagrangian $\mathcal{L} : \Phi \times L^2(0, T; H_0^1(0, 1)) \rightarrow \mathbb{R}$ defined by*

$$\mathcal{L}(\varphi, \lambda) = \frac{1}{2}a(\varphi, \varphi) + b(\varphi, \lambda) - l(\varphi). \quad (25)$$

- (iii) *The optimal function φ is the minimizer of \hat{J}^* over Φ while the optimal function $\lambda \in L^2(0, T; H_0^1(0, 1))$ is the state of the controlled wave equation (1) in the weak sense (associated to the control $-\varphi \mathbf{1}_{Q_T}$).*

PROOF - We easily check that the bilinear form a is continuous over $\Phi \times \Phi$, symmetric and positive and that the bilinear form b is continuous over $\Phi \times L^2(0, T; H_0^1(0, 1))$. Furthermore, the continuity of the linear form l over Φ is a direct consequence of the generalized observability inequality (11):

$$|l(\varphi)| \leq \|(y_0, y_1)\|_{\mathbf{V}} \sqrt{C \max(1, \eta^{-1})} \|\varphi\|_{\Phi}, \quad \forall \varphi \in \Phi.$$

Therefore, the well-posedness of the mixed formulation is a consequence of the following two properties (see [5]):

- a is coercive on $\mathcal{N}(b)$, where $\mathcal{N}(b)$ denotes the kernel of b :

$$\mathcal{N}(b) = \{ \varphi \in \Phi \text{ such that } b(\varphi, \lambda) = 0 \text{ for every } \lambda \in L^2(0, T; H_0^1(0, 1)) \};$$

- b satisfies the usual "inf-sup" condition over $\Phi \times L^2(0, T; H_0^1(0, 1))$: there exists $\delta > 0$ such that

$$\inf_{\lambda \in L^2(0, T; H_0^1(0, 1))} \sup_{\varphi \in \Phi} \frac{b(\varphi, \lambda)}{\|\varphi\|_{\Phi} \|\lambda\|_{L^2(0, T; H_0^1(0, 1))}} \geq \delta. \quad (26)$$

From the definition of a , the first point is clear : for all $\varphi \in \mathcal{N}(b) = W$, $a(\varphi, \varphi) = \|\varphi\|_W^2$. Let us check the inf-sup condition (26). For any fixed $\lambda_0 \in L^2(0, T; H_0^1(0, 1))$, we define the (unique) element φ_0 such that $L\varphi_0 = -\Delta\lambda_0$ in Q_T and such that $\varphi_0(\cdot, 0) = 0$ in $L^2(0, 1)$ and $\varphi_{0,t}(\cdot, 0) = 0$ in $H^{-1}(0, 1)$. φ_0 is therefore solution of the wave equation with source term $-\Delta\lambda_0 \in L^2(0, T; H^{-1}(0, 1))$, null Dirichlet boundary condition and zero initial state. We then use the following estimate (see for instance Chapter 1 in [19]): there exists a constant $C_{\Omega, T} > 0$ such that

$$\|\varphi_0\|_{L^2(Q_T)} \leq C_{\Omega, T} \|\Delta\lambda_0\|_{L^2(0, T; H^{-1}(0, 1))} \leq C_{\Omega, T} \|\lambda_0\|_{L^2(0, T; H_0^1(0, 1))}. \quad (27)$$

Consequently, $\varphi_0 \in \Phi$. In particular, we have $b(\varphi_0, \lambda_0) = \|\lambda_0\|_{L^2(0, T; H_0^1(0, 1))}^2$ and

$$\begin{aligned} \sup_{\varphi \in \Phi} \frac{b(\varphi, \lambda_0)}{\|\varphi\|_{\Phi} \|\lambda_0\|_{L^2(Q_T)}} &\geq \frac{b(\varphi_0, \lambda_0)}{\|\varphi_0\|_{\Phi} \|\lambda_0\|_{L^2(Q_T)}} \\ &= \frac{\|\lambda_0\|_{L^2(0, T; H_0^1(0, 1))}^2}{\left(\|\varphi_0\|_{L^2(Q_T)}^2 + \eta \|\lambda_0\|_{L^2(0, T; H_0^1(0, 1))}^2\right)^{\frac{1}{2}} \|\lambda_0\|_{L^2(0, T; H_0^1(0, 1))}}. \end{aligned}$$

Combining the above two inequalities, we obtain

$$\sup_{\varphi_0 \in \Phi} \frac{b(\varphi_0, \lambda_0)}{\|\varphi_0\|_{\Phi} \|\lambda_0\|_{L^2(0, T; H_0^1(0, 1))}} \geq \frac{1}{\sqrt{C_{\Omega, T}^2 + \eta}}$$

and, hence, (26) holds with $\delta = (C_{\Omega, T}^2 + \eta)^{-\frac{1}{2}}$.

The point (ii) is due to the symmetry and to the positivity of the bilinear form a . (iii). The equality $b(\varphi, \lambda) = 0$ for all $\lambda \in L^2(0, T; H_0^1(0, 1))$ implies that $L\varphi = 0$ as an $L^2(0, T; H^{-1}(0, 1))$ function, so that if $(\varphi, \lambda) \in \Phi \times L^2(0, T; H_0^1(0, 1))$ solves the mixed formulation, then $\varphi \in W$ and $\mathcal{L}(\varphi, \lambda) = \hat{J}^*(\varphi)$. Finally, the first equation of the mixed formulation reads as follows :

$$\iint_{q_T} \varphi \bar{\varphi} dx dt + \int_0^T \langle L\bar{\varphi}, \lambda \rangle_{H^{-1}, H_0^1} dt = l(\bar{\varphi}), \quad \forall \bar{\varphi} \in \Phi,$$

or equivalently, since the control of minimal $L^2(q_T)$ norm is given by $v = -\varphi 1_{q_T}$,

$$\iint_{Q_T} -v 1_{q_T} \bar{\varphi} dx dt + \int_0^T \langle L\bar{\varphi}, \lambda \rangle_{H^{-1}, H_0^1} dt = l(\bar{\varphi}), \quad \forall \bar{\varphi} \in \Phi.$$

But this means that $\lambda \in L^2(0, T; H_0^1(0, 1))$ is solution of the wave equation in the transposition sense. Since $(y_0, y_1) \in \mathbf{V}$ and $v \in L^2(q_T)$, λ must coincide with the unique weak solution to (1). \square

Therefore, Theorem 3.1 reduces the search of the control of square minimal norm to the resolution of the mixed formulation (24), or equivalently to the search of the saddle point for \mathcal{L} . In general, it is very convenient (and actually necessary in Section 3.2) to "augment" the Lagrangian (see [14]), and consider instead the Lagrangian \mathcal{L}_r defined for any $r > 0$ by

$$\begin{cases} \mathcal{L}_r(\varphi, \lambda) := \frac{1}{2} a_r(\varphi, \varphi) + b(\varphi, \lambda) - l(\varphi), \\ a_r(\varphi, \varphi) := a(\varphi, \varphi) + r \|L\varphi\|_{L^2(0, T; H^{-1}(0, 1))}^2. \end{cases}$$

Since $a(\varphi, \varphi) = a_r(\varphi, \varphi)$ on W , the Lagrangian \mathcal{L} and \mathcal{L}_r share the same saddle-point.

Remark 2 The estimate (11) may also be used to extend the work [9] to the non-cylindrical situation. Reference [9] considers the pair (y, v) solution of (1-3) which minimize the following L^2 -weighted functional

$$J(y, v) := \frac{1}{2} \iint_{Q_T} \rho^2(x, t) |y|^2 dx dt + \frac{1}{2} \iint_{q_T} \rho_0^2(x, t) |v|^2 dx dt$$

for any weights $\rho, \rho_0 \in C(\overline{Q_T}, \mathbb{R}_+^*)$. Assuming $|\rho|$ and $|\rho_0|$ uniformly positive by below, the unique minimizer (y, v) is expressed in term of the auxiliary variable $p \in P := \{p : \rho^{-1} Lp \in L^2(Q_T), \rho_0^{-1} p \in L^2(q_T), p = 0 \text{ on } \Sigma_T\}$ as follows :

$$y = -\rho^{-2} Lp, \quad v = \rho_0^{-2} p 1_{q_T} \quad \text{on } Q_T$$

where p is the solution of the variational formulation

$$\iint_{Q_T} \rho^{-2} Lp Lq dx dt + \iint_{q_T} \rho_0^{-2} p q dx dt = \int_0^1 y^1 q(\cdot, 0) dx - \langle y^0, q_t(\cdot, 0) \rangle_{H_0^1(0,1), H^{-1}(0,1)}, \quad \forall q \in P.$$

The well-posedness of this formulation is given by the estimate (11).

3.2 Dual problem of the extremal problem (23)

The mixed formulation allows to solve simultaneously the dual variable φ , argument of the conjugate functional (23), and the Lagrangian multiplier λ . Since λ turns out to be the controlled state of (1), we may qualify λ as the primal variable of the controllability problem. We derive in this section the corresponding extremal problem involving only that variable λ .

For any $r > 0$, let us define the linear operator A_r from $L^2(0, T; H_0^1(0, 1))$ into $L^2(0, T; H_0^1(0, 1))$ by

$$A_r \lambda := -\Delta^{-1}(L\varphi), \quad \forall \lambda \in L^2(0, T; H_0^1(0, 1))$$

where $\varphi \in \Phi$ is the unique solution to

$$a_r(\varphi, \bar{\varphi}) = b(\bar{\varphi}, \lambda), \quad \forall \bar{\varphi} \in \Phi. \quad (28)$$

Notice that the assumption $r > 0$ is needed here in order to guarantee the well-posedness of (28). Precisely, for any $r > 0$, the form a_r defines a norm equivalent to the norm on φ .

We have the following important lemma :

LEMMA 3.1 For any $r > 0$, the operator A_r is a strongly elliptic, symmetric isomorphism from $L^2(0, T; H_0^1(0, 1))$ into $L^2(0, T; H_0^1(0, 1))$.

PROOF- From the definition of a_r , we easily get that $\|A_r \lambda\|_{L^2(0, T; H_0^1(0, 1))} \leq r^{-1} \|\lambda\|_{L^2(0, T; H_0^1(0, 1))}$ and the continuity of A_r . Next, consider any $\lambda' \in L^2(0, T; H_0^1(0, 1))$ and denote by φ' the corresponding unique solution of (28) so that $A_r \lambda' := -\Delta^{-1}(L\varphi')$. Relation (28) with $\bar{\varphi} = \varphi'$ then implies that

$$\int_0^T \langle A_r \lambda', \lambda \rangle_{H_0^1(0,1), H_0^1(0,1)} dt = a_r(\varphi, \varphi') \quad (29)$$

and therefore the symmetry and positivity of A_r . The last relation with $\lambda' = \lambda$ and the estimate (11) imply that A_r is also positive definite.

Finally, let us check the strong ellipticity of A_r , equivalently that the bilinear functional $(\lambda, \lambda') \rightarrow \int_0^T \langle A_r \lambda, \lambda' \rangle_{H_0^1(0,1), H_0^1(0,1)} dt$ is $L^2(0, T; H_0^1(0, 1))$ -elliptic. Thus we want to show that

$$\int_0^T \langle A_r \lambda, \lambda \rangle_{H_0^1(0,1), H_0^1(0,1)} dt \geq C \|\lambda\|_{L^2(0, T; H_0^1(0, 1))}^2, \quad \forall \lambda \in L^2(0, T; H_0^1(0, 1)) \quad (30)$$

for some positive constant C . Suppose that (30) does not hold; there exists then a sequence $\{\lambda_n\}_{n \geq 0}$ of $L^2(0, T; H_0^1(0, 1))$ such that

$$\|\lambda_n\|_{L^2(0, T; H_0^1(0, 1))} = 1, \quad \forall n \geq 0, \quad \text{and} \quad \lim_{n \rightarrow \infty} \int_0^T \langle A_r \lambda_n, \lambda_n \rangle_{H_0^1(0, 1), H_0^1(0, 1)} dt = 0.$$

Let us denote by φ_n the solution of (28) corresponding to λ_n . From (29), we then obtain that

$$\lim_{n \rightarrow \infty} \|L\varphi_n\|_{L^2(0, T; H^{-1}(0, 1))} = 0, \quad \lim_{n \rightarrow +\infty} \|\varphi_n\|_{L^2(Q_T)} = 0 \quad (31)$$

and thus $\lim_{n \rightarrow \infty} \int_0^T \langle -\Delta^{-1}(L\varphi), \lambda_n \rangle_{H_0^1(0, 1), H_0^1(0, 1)} dt = 0$ for all $\varphi \in \Phi$ (and so the $L^2(0, T; H_0^1(0, 1))$ -weak-convergence of λ_n toward 0).

From (28) with $\varphi = \varphi_n$ and λ_n , we have

$$\int_0^T \langle -r\Delta^{-1}(L\varphi_n) - \lambda_n, -\Delta^{-1}(L\bar{\varphi}) \rangle_{H_0^1(0, 1), H_0^1(0, 1)} dt + \iint_{Q_T} \varphi_n \bar{\varphi} dx dt = 0, \quad \forall \bar{\varphi} \in \Phi. \quad (32)$$

We define the sequence $\{\bar{\varphi}_n\}_{n \geq 0}$ as follows :

$$\begin{cases} L\bar{\varphi}_n = r L\varphi_n + \Delta\lambda_n, & \text{in } Q_T, \\ \bar{\varphi}_n(0, \cdot) = \bar{\varphi}_n(1, \cdot) = 0, & \text{in } (0, T), \\ \bar{\varphi}_n(\cdot, 0) = \bar{\varphi}_{n,t}(\cdot, 0) = 0, & \text{in } (0, 1) \end{cases}$$

so that, for all n , $\bar{\varphi}_n$ is the solution of the wave equation with zero initial data and source term $r L\varphi_n + \Delta\lambda_n$ in $L^2(0, T; H^{-1}(0, 1))$. Using again (27), we get $\|\bar{\varphi}_n\|_{L^2(Q_T)} \leq C_{\Omega, T} \|r L\varphi_n + \Delta\lambda_n\|_{L^2(0, T; H^{-1}(0, 1))}$, so that $\bar{\varphi}_n \in \Phi$. Then, using (32), we get

$$\| -r\Delta^{-1}(L\varphi_n) - \lambda_n \|_{L^2(0, T; H_0^1(0, 1))} \leq C_{\Omega, T} \|\varphi_n\|_{L^2(Q_T)}.$$

Then, from (31), we conclude that $\lim_{n \rightarrow +\infty} \|\lambda_n\|_{L^2(0, T; H_0^1(0, 1))} = 0$ leading to a contradiction and to the strong ellipticity of the operator A_r . \square

The introduction of the operator A_r is motivated by the following proposition :

PROPOSITION 3.1 *Let $\varphi_0 \in \Phi$ the unique solution of*

$$a_r(\varphi_0, \bar{\varphi}) = l(\bar{\varphi}), \quad \forall \bar{\varphi} \in \Phi$$

*and let $J^{**} : L^2(0, T; H_0^1(0, 1)) \rightarrow L^2(0, T; H_0^1(0, 1))$ the functional defined by*

$$J^{**}(\lambda) = \frac{1}{2} \int_0^T \langle A_r \lambda, \lambda \rangle_{H_0^1(0, 1), H_0^1(0, 1)} dt - b(\varphi_0, \lambda).$$

The following equality holds :

$$\sup_{\lambda \in L^2(0, T; H_0^1(0, 1))} \inf_{\varphi \in \Phi} \mathcal{L}_r(\varphi, \lambda) = - \inf_{\lambda \in L^2(0, T; H_0^1(0, 1))} J^{**}(\lambda) + \mathcal{L}_r(\varphi_0, 0).$$

PROOF- For any $\lambda \in L^2(0, T; H_0^1(0, 1))$, let us denote by $\varphi_\lambda \in \Phi$ the minimizer of $\varphi \rightarrow \mathcal{L}_r(\varphi, \lambda)$. φ_λ satisfies the equation

$$a_r(\varphi_\lambda, \bar{\varphi}) + b(\bar{\varphi}, \lambda) = l(\bar{\varphi}), \quad \forall \bar{\varphi} \in \Phi$$

and can be decomposed as follows : $\varphi_\lambda = \psi_\lambda + \varphi_0$ where $\psi_\lambda \in \Phi$ solves

$$a_r(\psi_\lambda, \bar{\varphi}) + b(\bar{\varphi}, \lambda) = 0, \quad \forall \bar{\varphi} \in \Phi.$$

We then have

$$\begin{aligned} \inf_{\varphi \in \Phi} \mathcal{L}_r(\varphi, \lambda) &= \mathcal{L}_r(\varphi_\lambda, \lambda) = \mathcal{L}_r(\psi_\lambda + \varphi_0, \lambda) \\ &= \frac{1}{2} a_r(\psi_\lambda + \varphi_0, \psi_\lambda + \varphi_0) + b(\psi_\lambda + \varphi_0, \lambda) - l(\psi_\lambda + \varphi_0) \\ &:= X_1 + X_2 + X_3 \end{aligned}$$

with

$$\begin{cases} X_1 = \frac{1}{2} a_r(\psi_\lambda, \psi_\lambda) + b(\psi_\lambda, \lambda) + b(\varphi_0, \lambda) \\ X_2 = a_r(\psi_\lambda, \varphi_0) - l(\psi_\lambda), \quad X_3 = \frac{1}{2} a_r(\varphi_0, \varphi_0) - l(\varphi_0). \end{cases}$$

From the definition of φ_0 , $X_2 = 0$ while $X_3 = \mathcal{L}_r(\varphi_0, 0)$. Eventually, from the definition of ψ_λ ,

$$X_1 = -\frac{1}{2} a_r(\psi_\lambda, \psi_\lambda) + b(\varphi_0, \lambda) = -\frac{1}{2} \int_0^T \langle A_r \lambda, \lambda \rangle_{H^1, H^1} dt + b(\varphi_0, \lambda)$$

and the result follows. \square

From the ellipticity of the operator A_r , the minimization of the functional J^{**} over $L^2(0, T, H_0^1)$ is well-posed. It is interesting to note that with this extremal problem involving only λ , we are coming to the primal variable, controlled solution of (1) (see Theorem 3.1, (iii)). Due to the constraint (3), the direct minimization of the null controllability problem by a penalty method with respect to the controlled state is usually avoided in practice. Here, any constraint equality is assigned to the variable λ .

From the symmetry and ellipticity of the operator A_r , the conjugate gradient algorithm is very appropriate to minimize J^{**} , and consequently solve the mixed formulation (24). The conjugate gradient algorithm reads as follows :

(i) Let $\lambda^0 \in L^2(0, T; H_0^1(0, 1))$ be a given function.

(ii) Compute $\bar{\varphi}^0 \in \Phi$ solution to

$$a_r(\bar{\varphi}^0, \bar{\varphi}) + b(\bar{\varphi}, \lambda^0) = l(\bar{\varphi}), \quad \forall \bar{\varphi} \in \Phi$$

and $g^0 = -\Delta^{-1}(L \bar{\varphi}^0)$ then set $w^0 = g^0$.

(iii) For $n \geq 0$, assuming that λ^n, g^n and w^n are known, compute $\bar{\varphi}^n \in \Phi$ solution to

$$a_r(\bar{\varphi}^n, \bar{\varphi}) = b(\bar{\varphi}, w^n), \quad \forall \bar{\varphi} \in \Phi$$

and $\bar{g}^n = -\Delta^{-1}(L \bar{\varphi}^n)$ and then

$$\rho_n = \|g^n\|_{L^2(0, T; H_0^1(0, 1))}^2 / (\bar{g}^n, w^n)_{L^2(0, T; H_0^1(0, 1))}.$$

Update λ^n and g^n by

$$\lambda^{n+1} = \lambda^n - \rho_n w^n, \quad g^{n+1} = g^n - \rho_n \bar{g}^n.$$

If $\|g^{n+1}\|_{L^2(0, T; H_0^1(0, 1))} / \|g^0\|_{L^2(0, T; H_0^1(0, 1))} \leq \varepsilon$, take $\lambda = \lambda^{n+1}$. Else, compute

$$\gamma_n = \|g^{n+1}\|_{L^2(0, T; H_0^1(0, 1))}^2 / \|g^n\|_{L^2(0, T; H_0^1(0, 1))}^2$$

and update w^n via

$$w^{n+1} = g^{n+1} + \gamma_n w^n.$$

Do $n = n + 1$ and return to step (iii).

As mentioned in [15] where this approach is discussed at length for Navier-Stokes type systems, this algorithm can be viewed as a sophisticated version of Arrow-Hurwicz-Uzawa type method.

Concerning the speed of convergence of the conjugate gradient algorithm (i)-(iii), it follows from for instance [12] that

$$\|\lambda^n - \lambda\|_{L^2(0,T;H_0^1(0,1))} \leq 2\sqrt{\nu(A_r)} \left(\frac{\sqrt{\nu(A_r)} - 1}{\sqrt{\nu(A_r)} + 1} \right)^n \|\lambda^0 - \lambda\|_{L^2(0,T;H_0^1(0,1))}, \quad \forall n \geq 1$$

where λ minimizes $J^{\star\star}$. $\nu(A_r) = \|A_r\| \|A_r^{-1}\|$ denotes the condition number of the operator A_r .

Eventually, once the above algorithm has converged we can compute $\varphi \in \Phi$ as solution of

$$a_r(\varphi, \bar{\varphi}) + b(\bar{\varphi}, \lambda) = l(\bar{\varphi}), \quad \forall \bar{\varphi} \in \Phi.$$

4 Numerical approximation and experiments

4.1 Some domains q_T

Let us first describe the domains $q_T \subset Q_T := (0, 1) \times (0, T)$ in which the control is supported we shall use in our numerical experiments.

Let $\gamma_T^i : (0, T) \rightarrow (0, 1)$ be four C^∞ functions defined as follows :

$$\gamma_T^0(t) = \frac{3}{10}, \quad t \in (0, T), \quad (33)$$

$$\gamma_T^1(t) = \frac{1}{2} + \frac{1}{10} \cos\left(\frac{\pi t}{T}\right), \quad t \in (0, T), \quad (34)$$

$$\gamma_T^2(t) = \frac{\beta - \alpha}{T} t + \alpha, \quad t \in (0, T), \quad (35)$$

$$\gamma_T^3(t) = \frac{1}{2} + \frac{1}{4} \cos\left(\frac{8\pi t}{T}\right), \quad t \in (0, T). \quad (36)$$

In what follows we choose in (35) $\alpha = 0.2$ and $\beta = 0.8$.

For each $i \in \{0, 1, 2, 3\}$, let $a_T^i, b_T^i : (0, T) \rightarrow (0, 1)$ be two functions defined by

$$a_T^i(t) = \gamma_T^i(t) - \delta_0, \quad b_T^i(t) = \gamma_T^i(t) + \delta_0, \quad t \in (0, T). \quad (37)$$

for some $\delta_0 > 0$ small enough. We then define the corresponding domains q_T^i as follows :

$$q_T^i = \{(x, t) \in Q_T; a_T^i(t) < x < b_T^i(t), t \in (0, T)\}, \quad i \in \{0, 1, 2, 3\}. \quad (38)$$

Remark that, in the definition of a_T^i and b_T^i , we may consider time-dependent value for δ_0 . Figure 2 display the domains q_T^i defined by (38) with the controllability time $T = 2.2$ and $\delta_0 = 10^{-1}$. We easily check, that for any $T > 2$, these domains satisfy the geometric condition of Proposition 2.1.

4.2 Discretization

We now turn to the discretization of the mixed formulation (24) assuming $r > 0$.

Let then Φ_h and M_h be two finite dimensional spaces parametrized by the variable h such that

$$\Phi_h \subset \Phi, \quad M_h \subset L^2(0, T; H_0^1(0, 1)), \quad \forall h > 0.$$

Then, we can introduce the following approximated problems : find $(\varphi_h, \lambda_h) \in \Phi_h \times M_h$ solution of

$$\begin{cases} a_r(\varphi_h, \bar{\varphi}_h) + b(\bar{\varphi}_h, \lambda_h) &= l(\bar{\varphi}_h), & \forall \bar{\varphi}_h \in \Phi_h \\ b(\varphi_h, \bar{\lambda}_h) &= 0, & \forall \bar{\lambda}_h \in M_h. \end{cases} \quad (39)$$

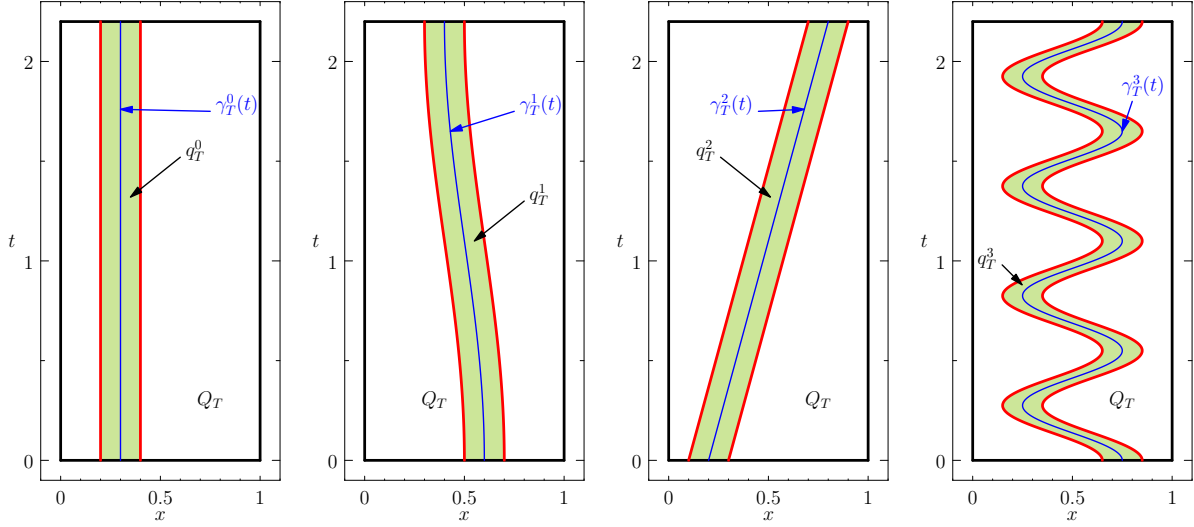


Figure 2: The time dependent domains Q_T^i , $i \in \{0, 1, 2, 3\}$ defined by (38).

The well-posedness of this mixed formulation is again a consequence of two properties : the coercivity of the bilinear form a_r on the subset $\mathcal{N}_h(b) = \{\varphi_h \in \Phi_h; b(\varphi_h, \lambda_h) = 0 \quad \forall \lambda_h \in M_h\}$. Actually, from the relation

$$a_r(\varphi, \varphi) \geq \frac{r}{\eta} \|\varphi\|_{\Phi}^2, \quad \forall \varphi \in \Phi$$

the form a_r is coercive on the full space Φ , and so *a fortiori* on $\mathcal{N}_h(b) \subset \Phi_h \subset \Phi$. The second property is a discrete inf-sup condition : there exists $\delta_h > 0$ such that

$$\inf_{\lambda_h \in M_h} \sup_{\varphi_h \in \Phi_h} \frac{b(\varphi_h, \lambda_h)}{\|\varphi_h\|_{\Phi_h} \|\lambda_h\|_{M_h}} \geq \delta_h. \quad (40)$$

For any fixed h , the spaces M_h and Φ_h are of finite dimension so that the infimum and supremum in (40) are reached: moreover, from the property of the bilinear form a_r , it is standard to prove that δ_h is strictly positive (see Section 4.5). Consequently, for any fixed $h > 0$, there exists a unique couple (φ_h, λ_h) solution of (39). On the other hand, the property $\inf_h \delta_h > 0$ is in general difficult to prove and depends strongly on the choice made for the approximated spaces M_h and Φ_h . We shall analyze numerically this property in Section 4.5.

The finite dimensional and conformal space Φ_h must be chosen such that $L\varphi_h$ belongs to $L^2(0, T, H^{-1}(0, 1))$ for any $\varphi_h \in \Phi_h$. This is guaranteed for instance as soon as φ_h possesses second-order derivatives in $L_{loc}^2(Q_T)$. Therefore, a conformal approximation based on standard triangulation of Q_T requires spaces of functions continuously differentiable with respect to both variables x and t .

We introduce a triangulation \mathcal{T}_h such that $\overline{Q_T} = \cup_{K \in \mathcal{T}_h} K$ and we assume that $\{\mathcal{T}_h\}_{h>0}$ is a regular family. We note

$$h := \max\{\text{diam}(K), K \in \mathcal{T}_h\}$$

where $\text{diam}(K)$ denotes the diameter of K . Then, we introduce the space Φ_h as follows :

$$\Phi_h = \{\varphi_h \in \Phi_h \in C^1(\overline{Q_T}) : \varphi_h|_K \in \mathbb{P}(K) \quad \forall K \in \mathcal{T}_h, \varphi_h = 0 \text{ on } \Sigma_T\}$$

where $\mathbb{P}(K)$ denotes an appropriate space of polynomial functions in x and t . In this work, we consider for $\mathbb{P}(K)$ the reduced *Hsieh-Clough-Tocher* (HCT for short) C^1 -element. This is a so-called composite finite element and involves 9 degrees of freedom, namely the values of $\varphi_h, \varphi_{h,x}, \varphi_{h,t}$ on the

three vertices of each triangle K . We refer to [8] page 356 and to [2, 21] where the implementation is discussed.

We also define the finite dimensional space

$$M_h = \{\lambda_h \in C^0(\overline{Q_T}), \lambda_h|_K \in \mathbb{Q}(K) \quad \forall K \in \mathcal{T}_h, \lambda_h = 0 \text{ on } \Sigma_T\}$$

where $\mathbb{Q}(K)$ denotes the space of affine functions both in x and t on the element K . For any $h > 0$, we have $\Phi_h \subset \Phi$ and $M_h \subset L^2(0, T; H_0^1(0, 1))$.

For each combination of domains (q_T, Q_T) described in Section 4.1 we consider six levels of triangulations \mathcal{T}_h (numbered from $\sharp 0$ to $\sharp 5$, from coarser to finer). The number of triangles for some examples of domains q_T which will be used the experiments are summarized in Table 1. In Figure 3 we display the meshes $\sharp 1$ corresponding to geometries described in Figure 2.

\sharp Mesh	0	1	2	3	4	5
$q_{T=2.2}^0$	207	828	3 312	13 248	52 992	211 968
$q_{T=2}^0$	198	792	3 168	12 672	50 688	202 752
$q_{T=2.2}^1$	150	600	2 400	9 600	38 400	153 600
$q_{T=2.2}^2$	179	716	2 864	11 456	45 824	183 296
$q_{T=2}^2$	177	708	2 832	11 328	45 312	181 248
$q_{T=2.2}^3$	464	1 856	7424	29 696	118 784	475 136

Table 1: Number of triangles for different meshes and different control domains q_T^i

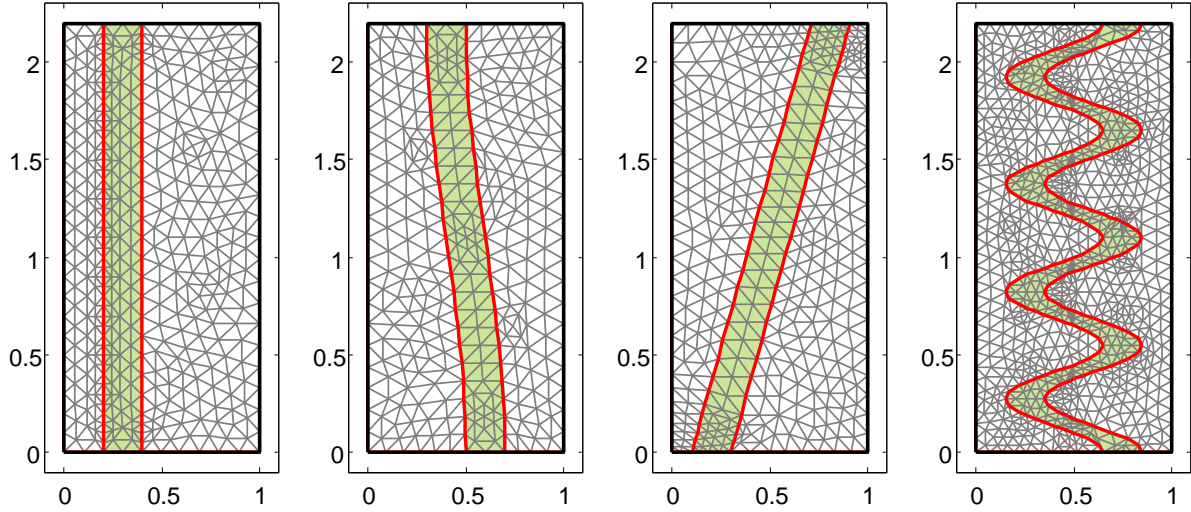


Figure 3: Meshes $\sharp 1$ associated with the domains $q_{T=2.2}^i : i = 0, 1, 2, 3$ from left to right.

4.3 Change of the norm $\|\cdot\|_{L^2(H^{-1})}$ over the discrete space Φ_h

In contrast to [10] where the boundary controllability is considered with the constraint $L\varphi = 0$ as an $L^2(Q_T)$ function, the equality $L\varphi = 0$ in Φ is assumed in the weaker space $L^2(0, T; H^{-1}(0, 1))$. It is not straightforward to handle numerically the scalar product over H^{-1} which appears in the mixed formulation (39). However, at the finite dimensional level of the discretization, since all the norms are equivalent, a classical trick (see for instance [3, 4]) consists in replacing, for any fixed h , the norm $\|L\varphi_h\|_{L^2(0, T; H^{-1}(0, 1))}$ by the norm $\|L\varphi_h\|_{L^2(Q_T)}$, up to a constant.

In order to do that, first remark that if there exist two constants $C_0 > 0$ and $\alpha > 0$ such that

$$\|\psi_h\|_{L^2(Q_T)}^2 \geq C_0 h^\alpha \|\psi_h\|_{L^2(0,T;H_0^1(0,1))}^2, \quad \forall \psi_h \in \Phi_h \quad (41)$$

then a similar inequality it holds for weaker norms. More precisely, we have

$$\|\varphi_h\|_{L^2(0,T;H^{-1}(0,1))}^2 \geq C_0 h^\alpha \|\varphi_h\|_{L^2(Q_T)}^2, \quad \forall \varphi_h \in \Phi_h. \quad (42)$$

Indeed, to obtain (42) it suffices to take $\psi_h(\cdot, t) = (-\Delta)^{\frac{1}{2}} \varphi_h(\cdot, t)$ in (41). That gives

$$\int_0^T \left\| (-\Delta)^{-\frac{1}{2}} \varphi_h(\cdot, t) \right\|_{L^2(0,1)}^2 dt \geq C_0 h^\alpha \int_0^T \left\| (-\Delta)^{-\frac{1}{2}} \varphi_{h,x}(\cdot, t) \right\|_{L^2(0,1)}^2 dt.$$

Since $-\Delta$ is a self-adjoint positive operator and $\varphi_h \in \Phi_h \subset H_0^1(Q_T)$ we can integrate by parts in both hand-sides of the above inequality and hence we deduce estimate (42). We highlight that the term $C_0 h^\alpha$ (and so C_0 and α) does not depend on T .

Assuming that (41) (and consequently (42)) holds (the constants $C_0, \alpha > 0$ will be approximated numerically in Section 4.4), we may consider, for any fixed $h > 0$, the following equivalent definitions of the form $a_{r,h}$ and b_h over the finite dimensional spaces $\Phi_h \times \Phi_h$ and $\Phi_h \times M_h$ respectively :

$$a_{r,h} : \Phi_h \times \Phi_h \rightarrow \mathbb{R}, \quad a_{r,h}(\varphi_h, \overline{\varphi_h}) = a(\varphi_h, \overline{\varphi_h}) + r C_0 h^\alpha \iint_{Q_T} L \varphi_h L \overline{\varphi_h} dx dt \quad (43)$$

$$b_h : \Phi_h \times M_h \rightarrow \mathbb{R}, \quad b_h(\varphi_h, \lambda_h) = \iint_{Q_T} L \varphi_h \lambda_h dx dt. \quad (44)$$

Let $n_h = \dim \Phi_h, m_h = \dim M_h$ and let the real matrices $A_{r,h} \in \mathbb{R}^{n_h, n_h}, B_h \in \mathbb{R}^{m_h, n_h}, J_h \in \mathbb{R}^{m_h, m_h}$ and $L_h \in \mathbb{R}^{n_h, 1}$ be defined by

$$a_{r,h}(\varphi_h, \overline{\varphi_h}) = \langle A_{r,h} \{\varphi_h\}, \{\overline{\varphi_h}\} \rangle_{\mathbb{R}^{n_h}, \mathbb{R}^{n_h}}, \quad \forall \varphi_h, \overline{\varphi_h} \in \Phi_h, \quad (45)$$

$$b_h(\varphi_h, \lambda_h) = \langle B_h \{\varphi_h\}, \{\lambda_h\} \rangle_{\mathbb{R}^{m_h}, \mathbb{R}^{m_h}}, \quad \forall \varphi_h \in \Phi_h, \forall \lambda_h \in M_h, \quad (46)$$

$$\iint_{Q_T} \lambda_h \overline{\lambda_h} dx dt = \langle J_h \{\lambda_h\}, \{\overline{\lambda_h}\} \rangle_{\mathbb{R}^{m_h}, \mathbb{R}^{m_h}}, \quad \forall \lambda_h, \overline{\lambda_h} \in M_h, \quad (47)$$

$$l(\varphi_h) = \langle L_h, \{\varphi_h\} \rangle, \quad \forall \varphi_h \in \Phi_h \quad (48)$$

where $\{\varphi_h\} \in \mathbb{R}^{n_h, 1}$ denotes the vector associated to φ_h and $\langle \cdot, \cdot \rangle_{\mathbb{R}^{n_h}, \mathbb{R}^{n_h}}$ the usual scalar product over \mathbb{R}^{n_h} . With these notations, the problem (39) reads as follows : find $\{\varphi_h\} \in \mathbb{R}^{n_h, 1}$ and $\{\lambda_h\} \in \mathbb{R}^{m_h, 1}$ such that

$$\begin{pmatrix} A_{r,h} & B_h^T \\ B_h & 0 \end{pmatrix}_{\mathbb{R}^{n_h+m_h, n_h+m_h}} \begin{pmatrix} \{\varphi_h\} \\ \{\lambda_h\} \end{pmatrix}_{\mathbb{R}^{n_h+m_h, 1}} = \begin{pmatrix} L_h \\ 0 \end{pmatrix}_{\mathbb{R}^{n_h+m_h, 1}}. \quad (49)$$

The matrix $A_{r,h}$ as well as the mass matrix J_h are symmetric and positive definite for any $h > 0$ and any $r > 0$. On the other hand, the main matrix of order $m_h + n_h$ in (49) is symmetric but not positive definite. We use exact integration methods developed in [13] for the evaluation of the coefficients of the matrices. The system (49) is solved using the direct LU decomposition method.

Let us also mention that for $r = 0$, although the formulation (24) is well-posed, numerically, the corresponding matrix $A_{0,h}$ is not invertible. In the sequel, we shall consider strictly positive values for r .

Once the approximation φ_h is obtained, an approximation v_h of the control v is given by $v_h = -\varphi_h 1_{q_T} \in L^2(Q_T)$. The corresponding controlled state y_h may be obtained by solving (1) with standard forward approximation (we refer to [9], Section 4 where this is detailed). Here, since the controlled state is directly given by the multiplier λ , we simply use λ_h as an approximation of y and we do not report here the computation of y_h .

4.4 Numerical approximation of C_0 and α in (42).

In order to approximate the values of the constants C_0 , α appearing in (41)-(42) we consider the following problem :

$$\text{find } \alpha > 0 \text{ and } C_0 > 0 \text{ such that } \sup_{\varphi_h \in \Phi_h} \frac{\|\varphi_h\|_{L^2(0,T;H_0^1(0,1))}^2}{\|\varphi_h\|_{L^2(Q_T)}^2} \leq \frac{1}{C_0 h^\alpha}, \quad \forall h > 0. \quad (50)$$

Since Φ_h is a finite dimensional space, the supremum is, for any fixed $h > 0$, the solution of the following eigenvalue problem :

$$\forall h > 0, \quad \gamma_h = \sup \left\{ \gamma : K_h \{\psi_h\} = \gamma \bar{J}_h \{\psi_h\}, \quad \forall \{\psi_h\} \in \mathbb{R}^{m_h} \setminus \{0\} \right\} \quad (51)$$

where $K_h \in \mathbb{R}^{n_h, n_h}$ and $\bar{J}_h \in \mathbb{R}^{n_h, n_h}$ are the matrices defined by

$$\begin{aligned} \langle K_h \{\psi_h\}, \{\bar{\psi}_h\} \rangle_{\mathbb{R}^{n_h}, \mathbb{R}^{n_h}} &= \iint_{Q_T} \psi_{h,x} \bar{\psi}_{h,x} dx dt, & \forall \psi_h, \bar{\psi}_h \in \Phi_h, \\ \langle \bar{J}_h \{\psi_h\}, \{\bar{\psi}_h\} \rangle_{\mathbb{R}^{n_h}, \mathbb{R}^{n_h}} &= \iint_{Q_T} \psi_h \bar{\psi}_h dx dt, & \forall \psi_h, \bar{\psi}_h \in \Phi_h. \end{aligned}$$

We then can choose C_0 and α in (50) such that $C_0 h^\alpha = \gamma_h^{-1}$, where γ_h solves the problem (51). Figure 4 displays γ_h^{-1} corresponding to the matrices K_h and \bar{J}_h associated to the domains Q_T and q_T^0 for the six levels of mesh and $T = 2.2$. The values of constants C_0 and α which provide the best fitting are $C_0 \approx 1.48 \times 10^{-2}$ and $\alpha = 2.1993$. As expected, we also check that the constant γ_h (and so C_0 and α) does not depend on T nor on the controllability domain. From now on, we use these numerical values in the bilinear form $a_{r,h}$ defined by (43).

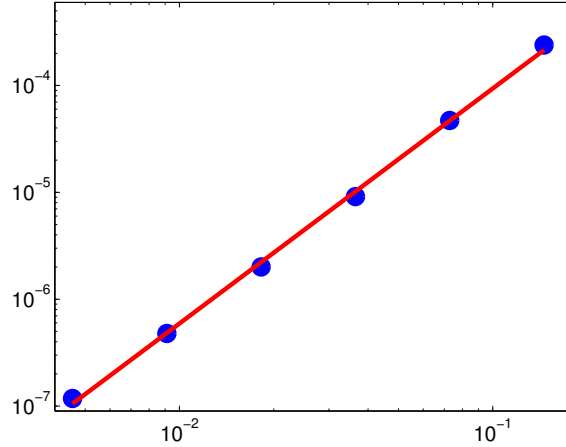


Figure 4: Values of γ_h^{-1} vs. h (\bullet). The line represents $C_0 h^\alpha$ for $C_0 \approx 1.48 \times 10^{-2}$ and $\alpha \approx 2.1993$.

4.5 The discrete inf-sup test

In order to solve the mixed formulation (39), we first test numerically the discrete inf-sup condition (40). Taking $\eta = r > 0$ in (10) so that $a_{r,h}(\varphi, \bar{\varphi}) = (\varphi, \bar{\varphi})_\Phi$ for all $\varphi, \bar{\varphi} \in \Phi$, it is readily seen (see for instance [7]) that the discrete inf-sup constant satisfies

$$\delta_h := \inf \left\{ \sqrt{\delta} : B_h A_{r,h}^{-1} B_h^T \{\lambda_h\} = \delta J_h \{\lambda_h\}, \quad \forall \{\lambda_h\} \in \mathbb{R}^{m_h} \setminus \{0\} \right\}. \quad (52)$$

As in the case of boundary controls (see [10]), the matrix $B_h A_{r,h}^{-1} B_h^T$ is symmetric and positive definite so that the real δ_h defined in term of the (generalized) eigenvalue problem (52) is, for any fixed value of the discretization parameter h , strictly positive. This eigenvalue problem is solved using the power iteration algorithm (assuming that the lowest eigenvalue is simple): for any $\{v_h^0\} \in \mathbb{R}^{n_h}$ such that $\|\{v_h^0\}\|_2 = 1$, compute for any $n \geq 0$, $\{\varphi_h^n\} \in \mathbb{R}^{n_h}$, $\{\lambda_h^n\} \in \mathbb{R}^{m_h}$ and $\{v_h^{n+1}\} \in \mathbb{R}^{m_h}$ iteratively as follows :

$$\begin{cases} A_{r,h}\{\varphi_h^n\} + B_h^T\{\lambda_h^n\} = 0 \\ B_h\{\varphi_h^n\} = -J_h\{v_h^n\} \end{cases}, \quad \{v_h^{n+1}\} = \frac{\{\lambda_h^n\}}{\|\{\lambda_h^n\}\|_2}.$$

The scalar δ_h defined by (52) is then given by : $\delta_h = \lim_{n \rightarrow \infty} (\|\{\lambda_h^n\}\|_2)^{-1/2}$.

Table 2 reports the values of δ_h for various mesh sizes h , for $r = 10^{-1}$ and $r = 10^{-3}$ and for $q_T = q_{2,2}^2$. As expected, we check that δ_h decreases as $h \rightarrow 0$ and increases as $r \rightarrow 0$. More importantly, this table suggests that the sequence δ_h remains uniformly bounded by below with respect to h . This property remains true for other control domains q_T , as emphasized by Figure 5.

# Mesh	1	2	3	4	5
h	7.18×10^{-2}	3.59×10^{-2}	1.79×10^{-2}	8.97×10^{-3}	4.49×10^{-3}
$r = 10^{-1}$	18.8171	17.5466	17.0642	16.8880	16.8254
$r = 10^3$	0.6981	0.8374	0.9246	0.9964	1.0826

Table 2: δ_h vs. h for $q_T = q_{2,2}^2$, $r = 10^{-1}$ and $r = 10^3$.

We may conclude that the finite elements we use do "pass" the discrete inf-sup test. As we shall see in the next section, this fact implies the convergence of the sequence φ_h and λ_h .

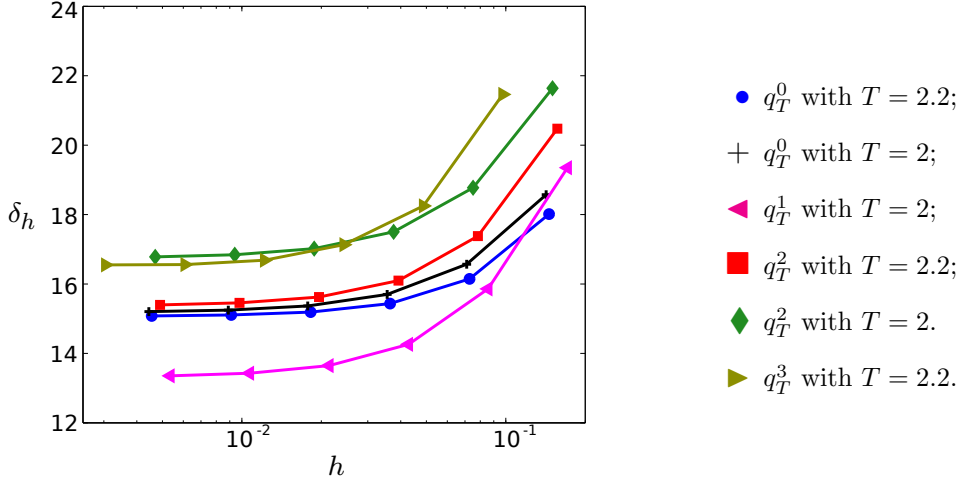


Figure 5: Values of δ_h vs. h for different control domains q_T^i and $r = 10^{-1}$.

4.6 Numerical experiments for $q_T = q_2^2$ and comparison with the explicit solution

We first consider the domain $q_T = q_2^2$ (see Figure 2) corresponding to an oblique band of length $2\delta_0 = 0.2$ and $T = 2$. We define also the following three initial data in $\mathbf{V} := H_0^1(0, 1) \times L^2(0, 1)$:

$$\text{(EX1)} \quad y_0(x) = \sin(\pi x), \quad y_1(x) = 0, \quad x \in (0, 1),$$

$$\text{(EX2)} \quad y_0(x) = e^{-500(x-0.8)^2}, \quad y_1(x) = 0, \quad x \in (0, 1),$$

$$\text{(EX3)} \quad y_0(x) = \frac{x}{\theta} 1_{(0,\theta)}(x) + \frac{1-x}{1-\theta} 1_{(\theta,1)}(x), \quad y_1(x) = 0, \quad \theta \in (0, 1), \quad x \in (0, 1).$$

In the case where the domain q_T depends on the variable t , there is no in general exact solution of the mixed formulation (24). However, we can obtain a semi-explicit representation (using Fourier decomposition) of the minimizer (φ_0, φ_1) of the conjugate functional J^* (see (8)), and consequently of the corresponding adjoint variable φ , the control of minimal square integrable norm $v = -\varphi 1_{q_T}$ and finally the controlled state y solution of (1-3). In practice, the obtention of the Fourier representation amounts to solve a symmetric linear system. We refer to the Appendix for the details. This allows to evaluate precisely the error $\|v - v_h\|_{L^2(q_T)}$ with respect to h and confirm the relevance of the method.

Table 3 and 4 collects some numerical values for $r = 10^{-1}$ and $r = 10^3$ respectively corresponding to the initial data (EX1). In the Tables, κ denotes the condition number associated to the linear system (49), independent of the initial data (y_0, y_1) . The convergence of $\|v - v_h\|_{L^2(q_T)}$, $\|L\varphi_h\|_{L^2(0,T;H^{-1}(0,1))}$ and $\|y - \lambda_h\|_{L^2(q_T)}$ toward zero as $h \searrow 0$ is clearly observed. This is fully in agreement with the uniform discrete inf-sup property we have observed in Section 4.5. We obtain the following rates of convergence with respect to h for $r = 10^{-1}$ and $r = 10^3$ respectively :

$$\begin{aligned} r = 10^{-1} : & \|v - v_h\|_{L^2(q_T)} \approx O(h^{1.3}), \|L\varphi_h\|_{L^2(0,T;H^{-1}(0,1))} \approx O(h^{1.3}), \|y - \lambda_h\|_{L^2(q_T)} \approx O(h^{1.94}) \\ r = 10^3 : & \|v - v_h\|_{L^2(q_T)} \approx O(h^{1.09}), \|L\varphi_h\|_{L^2(q_T)} \approx O(h^{1.04}), \|y - \lambda_h\|_{L^2(q_T)} \approx O(h^{2.01}). \end{aligned}$$

We refer to Figure 6 which highlights for $r = 10^{-1}$ the polynomial convergence of the sequences $\|y - \lambda_h\|_{L^2(q_T)}$ ("♦") and $\|v - v_h\|_{L^2(q_T^2)}$ ("•") with respect to h . The previous rates suggests that the value of the parameter r has a restricted influence.

# Mesh	1	2	3	4	5
h	7.18×10^{-2}	3.59×10^{-2}	1.79×10^{-2}	8.97×10^{-3}	4.49×10^{-3}
$\ v_h\ _{L^2(q_T)}$	5.370	5.047	4.893	4.815	4.776
$\ L\varphi_h\ _{L^2(0,T;H^{-1}(0,1))}$	2.286	9.43×10^{-1}	3.76×10^{-1}	1.5×10^{-1}	6.15×10^{-2}
$\ v - v_h\ _{L^2(q_T)}$	2.45×10^{-1}	9.65×10^{-2}	4.32×10^{-2}	2.29×10^{-2}	1.10×10^{-2}
$\ y - \lambda_h\ _{L^2(q_T)}$	5.63×10^{-3}	1.57×10^{-3}	4.04×10^{-4}	1.03×10^{-4}	2.61×10^{-5}
κ	2.46×10^7	2.67×10^8	2.96×10^9	3.03×10^{10}	3.08×10^{11}

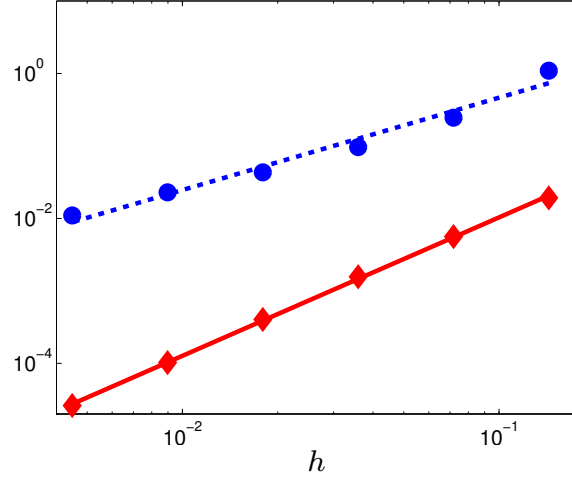
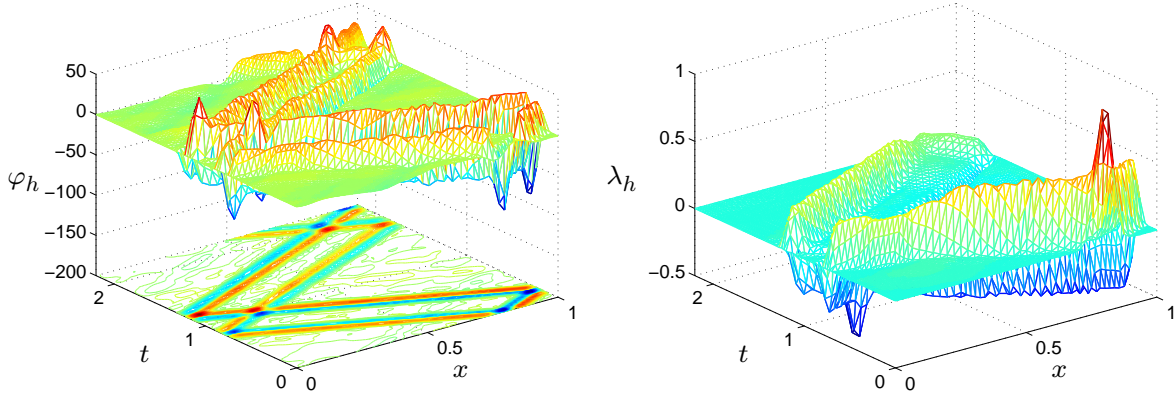
Table 3: Example EX1; $q_T = q_2^2$; $r = 10^{-1}$.

The convergence of the method is also observed for the initial data (EX2), mainly supported around $x = 0.8$ and the less regular data (EX3). Table 5 collects numerical values associated to (EX2), $q_T = q_2^2$ and $r = 10^{-1}$. We obtain the following rates :

$$\|v - v_h\|_{L^2(q_T)} \approx e^{5.85} h^{1.4}, \|L\varphi_h\|_{L^2(q_T)} \approx e^{7.96} h^{1.31}, \|y - \lambda_h\|_{L^2(q_T)} \approx e^{1.508} h^{1.62}$$

Figure 7 displays other Q_T the dual variable φ_h and the primal variable λ_h for $q_T = q_{2.2}^2$. The figures are obtained with the mesh #3. As expected, these variables are mainly concentrated along the characteristics starting from $x = 0.8$.

# Mesh	1	2	3	4	5
h	7.18×10^{-2}	3.59×10^{-2}	1.79×10^{-2}	8.97×10^{-3}	4.49×10^{-3}
$\ v_h\ _{L^2(Q_T)}$	4.1796	4.6185	4.7589	4.7557	4.7291
$\ L\varphi_h\ _{L^2(0,T;H^{-1}(0,1))}$	0.0391	0.0322	0.0162	0.0078	0.0037
$\ v - v_h\ _{L^2(Q_T)}$	2.4977	1.1341	0.5617	0.2418	0.1201
$\ y - \lambda_h\ _{L^2(Q_T)}$	9.23×10^{-2}	4.56×10^{-2}	7.70×10^{-3}	1.71×10^{-3}	4.46×10^{-4}
κ	6.12×10^8	1.44×10^{10}	1.51×10^{11}	1.55×10^{12}	1.54×10^{13}

Table 4: Example **EX1**; $q_T = q_{2.2}^2$; $r = 10^3$.Figure 6: Example **EX1**; $r = 10^{-1}$; $q_T = q_{2.2}^2$; Norms $\|v - v_h\|_{L^2(Q_T)}$ (●) and $\|y - \lambda_h\|_{L^2(Q_T)}$ (◆) vs. h .Figure 7: Example **EX2**; $r = 10^{-1}$; $q_T = q_{2.2}^2$: Functions φ_h (Left) and λ_h (Right) over Q_T .

Similarly, Table 6 gives the value corresponding to the third example **EX3**, here with $\theta = 1/2$. We obtain

$$\|v - v_h\|_{L^2(Q_T)} \approx e^{1.69} h^{0.53}, \quad \|L\varphi_h\|_{L^2(Q_T)} \approx e^{2.88} h^{0.56}, \quad \|y - \lambda_h\|_{L^2(Q_T)} \approx e^{-1.41} h^{1.32}.$$

Table 7 gives the numerical results for the Example **EX3** with $\theta = 1/3$. We get

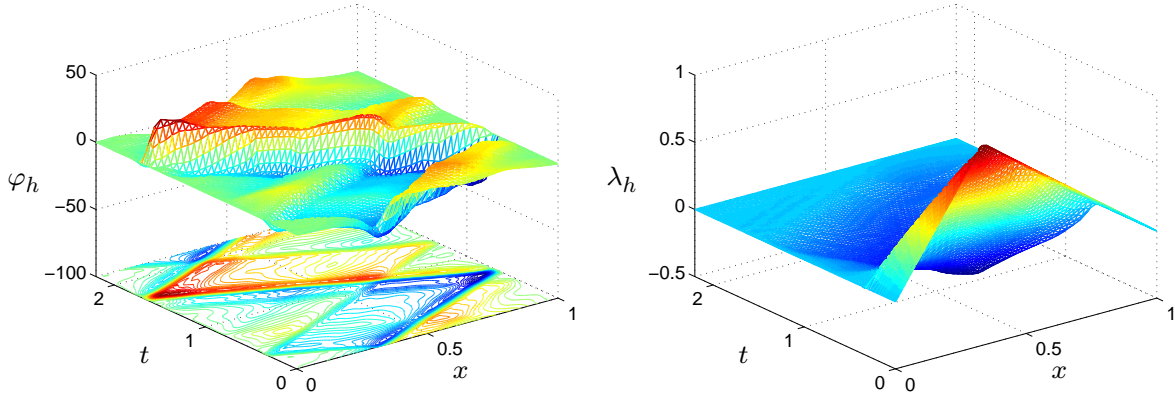
$$\|v - v_h\|_{L^2(Q_T)} \approx e^{1.54} h^{0.47}, \quad \|L\varphi_h\|_{L^2(Q_T)} \approx e^{2.91} h^{0.54}, \quad \|y - \lambda_h\|_{L^2(Q_T)} \approx e^{-1.52} h^{1.29}.$$

Figure 8 displays the dual variable φ_h and the primal variable λ_h for $q_T = q_{2.2}^2$ and **EX3** with $\theta = 1/3$. The figures are again plotted with the mesh #3.

# Mesh	1	2	3	4	5
h	7.18×10^{-2}	3.59×10^{-2}	1.79×10^{-2}	8.97×10^{-3}	4.49×10^{-3}
$\ v_h\ _{L^2(q_T)}$	4.8469	7.6514	10.9905	12.6256	12.9022
$\ L\varphi_h\ _{L^2(0,T;H^{-1}(0,1))}$	3.13×10^1	2.91×10^1	1.82×10^1	6.8984	1.9257
$\ v - v_h\ _{L^2(q_T)}$	8.4949	6.6975	3.2515	6.24×10^{-1}	5.31×10^{-2}
$\ y - \lambda_h\ _{L^2(Q_T)}$	5.98×10^{-2}	2.78×10^{-2}	8.97×10^{-3}	2.01×10^{-3}	5.38×10^{-4}

Table 5: Example **EX2**; $q_T = q_2^2$; $r = 10^{-1}$.

# Mesh	1	2	3	4	5
h	7.18×10^{-2}	3.59×10^{-2}	1.79×10^{-2}	8.97×10^{-3}	4.49×10^{-3}
$\ v_h\ _{L^2(q_T)}$	4.807	4.756	4.707	4.689	4.685
$\ L\varphi_h\ _{L^2(0,T;H^{-1}(0,1))}$	3.858	2.965	1.881	1.232	8.61×10^{-1}
$\ v - v_h\ _{L^2(q_T)}$	1.4382	8.73×10^{-1}	6.24×10^{-1}	4.24×10^{-1}	3.25×10^{-1}
$\ y - \lambda_h\ _{L^2(Q_T)}$	6.86×10^{-3}	3.55×10^{-3}	1.19×10^{-3}	4.64×10^{-4}	1.96×10^{-4}

Table 6: Example **EX3** with $\theta = 1/2$; $r = 10^{-1}$; $q_T = q_2^2$.Figure 8: Example **EX3** with $\theta = 1/3$; $r = 10^{-1}$; $q_T = q_{2,2}^2$: Functions φ_h (Left) and λ_h (Right).

4.7 Comparison of $\|v\|_{L^2(q_T)}$ for various domains q_T with the same measure

The optimization of the support domain q_T is particularly relevant in the time dependent situation. As a first step in this direction, we compare numerically in this section the $L^2(q_T)$ -norm of the control v_h for various domain q_T having the same measure. Along this section, we take $r = 10^{-1}$ and $T = 2.2$. The four domains we consider are $q_{T=2.2}^i$ for $i = 0, 1, 2, 3$ and are described in Section 4.1.

Table 8 reports the L^2 norms of $v_h = -\varphi_h 1_{q_T^i}$ obtained with the finer mesh (mesh #5, see Table 1) associated to each domain.

Figure 9 displays the dual variable φ_h and the primal one λ_h associated to the initial data **EX2** and control domains q_T^3 .

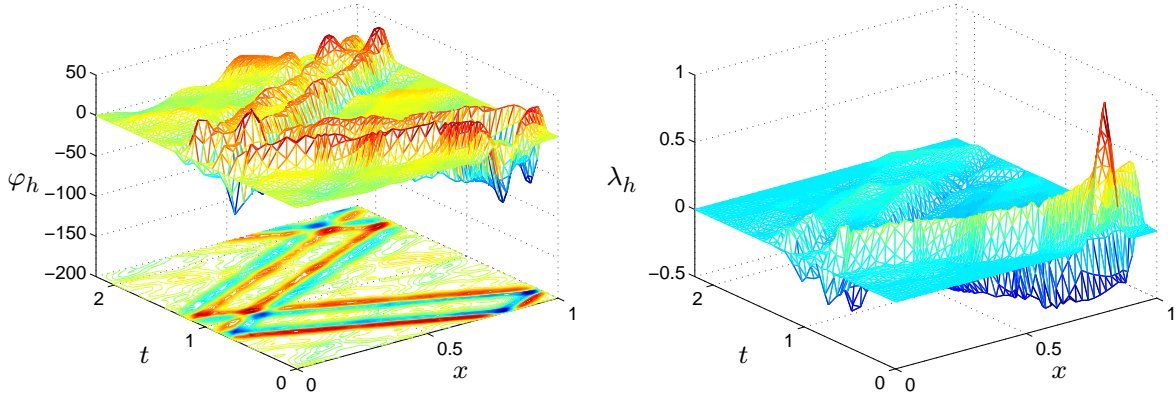
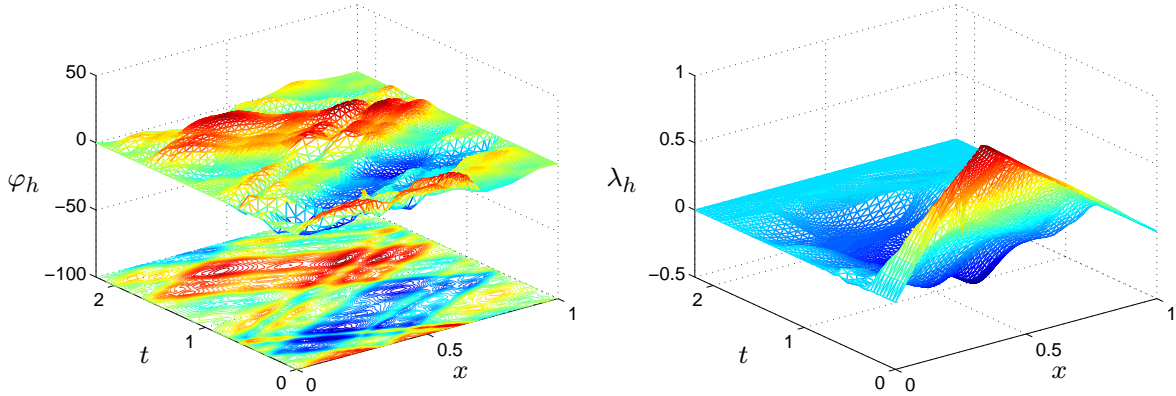
Figure 10 displays the dual variable φ_h and the primal one λ_h associated to the initial data **EX3**, $\theta = 1/3$ and control domains q_T^3 .

We remark that any of these domains provides minimal norm controls for every initial data **EX1-EX3**. In fact, we suspect that the domains minimizing the L^2 -norm of the control of minimal L^2 -norm are strongly connected with the set generated by the characteristics of the initial data. This questions will be investigated in a future study.

# Mesh	1	2	3	4	5
h	7.18×10^{-2}	3.59×10^{-2}	1.79×10^{-2}	8.97×10^{-3}	4.49×10^{-3}
$\ v_h\ _{L^2(q_T)}$	5.350	5.263	5.195	5.172	5.165
$\ L\varphi_h\ _{L^2(0,T;H^{-1}(0,1))}$	4.230	3.339	2.095	1.382	1.022
$\ v - v_h\ _{L^2(q_T)}$	1.3571	9.78×10^{-1}	6.91×10^{-1}	5.13×10^{-1}	3.69×10^{-1}
$\ y - \lambda_h\ _{L^2(Q_T)}$	7.12×10^{-3}	3.23×10^{-3}	1.19×10^{-3}	4.82×10^{-4}	2.12×10^{-4}

Table 7: Example **EX3** with $\theta = 1/3$; $r = 10^{-1}$; $q_T = q_2^2$.

Initial data	q_T^0	q_T^1	q_T^2	q_T^3
EX1	4.3677	3.8770	4.4808	5.5967
EX2	11.9994	12.0973	10.6268	11.2624
EX3 , $\theta = 1/3$	3.9946	4.5026	5.0132	5.0369

Table 8: L^2 -norm $\|v_h\|_{L^2(q_T)}$ for $q_T = q_{2,2}^i$, $i \in \{0, 3\}$ for initial data **EX1-EX3**.Figure 9: Example **EX2**: $q_T = q_{2,2}^3$ - Function φ_h (Left) and λ_h (Right) over Q_T .Figure 10: Example **EX3**, $\theta = 1/3$: $q_T = q_{2,2}^3$ - Function φ_h (Left) and λ_h (Right) over Q_T .

4.8 Behavior of the control as $\delta_0 \searrow 0$

The approach we have developed is valid for any support q_T satisfying the hypothesis of Proposition 2.1, in particular arbitrarily thin domain. In this Section we study numerically the evolution of the norm of the controls of minimal L^2 -norm supported in a time dependent domain q_T when the measure of these domains goes to 0. Precisely, we consider smaller and smaller values to the

parameter δ_0 defining the "thickness" of the domains q_T as specified by (37)-(38).

In Table 9 we give the L^2 and $L^2(H^{-1})$ norms of the controls obtained for the initial data **EX1** and control domains $q_{T=2}^2$ for $\delta_0 = \frac{10^{-1}}{2^i}$ for values of $i \in \{0, 1, 2, \dots, 6\}$. As $\delta_0 \searrow 0$, q_T^2 degenerates into the C^1 -curve γ_T^2 defined by (35); this curve satisfies the condition $|(\gamma_T^2)'(t)| < 1$ for all $t \in [0, T]$ assumed in [6] to prove the existence of $H^{-1}(\cup_{t \in (0, T)} \gamma(t) \times \{t\})$ controls.

The numerical values suggest that both norms of the controls are not uniformly bounded (by above) with respect to δ_0 ; this indicates that the L^2 -controllability of (1) with control supported on the curve $\gamma_{T=2}^2$ (see 35) does not hold. Similar behaviors are obtained for the other domains considered in Section 4.1 when $\delta_0 \searrow 0$. This does not contradict the result of [6] where the $H^{-1}(\cup_{t \in (0, T)} \gamma(t) \times \{t\})$ -controllability is proved in the limit situation.

δ_0	10^{-1}	$10^{-1}/2$	$10^{-1}/2^2$	$10^{-1}/2^3$	$10^{-1}/2^4$	$10^{-1}/2^5$	$10^{-1}/2^6$
# triangles	68 740	68 464	68 402	68 728	68 422	68 966	68 368
$\ v_h\ _{L^2(q_T)}$	4.830	7.330	11.574	18.805	29.735	47.315	123.970
$\ v_h\ _{L^2(H^{-1})}$	0.0035	0.0042	0.0066	0.0107	0.0170	0.0270	0.0704

Table 9: Example **EX1**; $q_T = q_2^2$; Norms of the control v_h obtained for the **EX1** for control domains q_2^2 for different values of δ_0 .

4.9 Other cases : Non constant velocity of propagation and $T < 2$

In order to illustrate our approach in a more challenging case we consider the wave equation with a non-constant velocity of propagation c and control supported in a time dependent domain :

$$\begin{cases} y_{tt} - (c(x)y_x)_x = v \mathbf{1}_{q_T}, & (x, t) \in Q_T \\ y(x, t) = 0, & (x, t) \in \Sigma_T \\ y(x, 0) = y_0(x), \quad y_t(x, 0) = y_1(x), & x \in (0, 1). \end{cases} \quad (53)$$

We take the velocity $c \in C^\infty(0, 1)$ given by

$$c(x) = \begin{cases} 1, & x \in [0, 0.45] \\ \in [1, 5], \quad (c'(x) > 0), & x \in (0.45, 0.55) \\ 5, & x \in [0.55, 1]. \end{cases} \quad (54)$$

Note that the Fourier expansion developed in the appendix does not apply in this case. Although the inequality (11) is open in this more general case, we observe that the solution of the mixed formulation (24) still provides convergent approximations $\{v_h\}$ of controls. Figure 11 depicts the dual variable φ_h and the primal variable λ_h corresponding to the approximation of the control for problem (53), for initial data given by **EX3** with $\theta = 1/3$ and control domain q_2^2 . The augmentation parameter is $r = 10^{-1}$.

Since the control acts in a time dependent domain, the geometric controllability condition can hold for values of the controllability time T which are smaller than 2 (we refer to [18]). Figure 12 displays φ_h and λ_h corresponding to the example **EX3** for $\theta = 1/3$, $T = 1$ and $q_T = q_1^2$. We mention that in this section the domains Q_T are discretized using uniform meshes formed by triangles of size $h \approx 10^{-2}$.

Another, even more challenging situation is the approximation of controls for problem (53) for shorter controllability times. In Figure 13 we display the results obtained for the initial data **EX3**, domain $q_{T=1}^2$ and the velocity of propagation is non constant in space and given by (54).

Analyzing the evolution of the norm of λ_h with respect to the time, in all the three examples considered in these section it seems to have the controllability, although the hypotheses of Proposition 2.1 are not completely fulfilled.

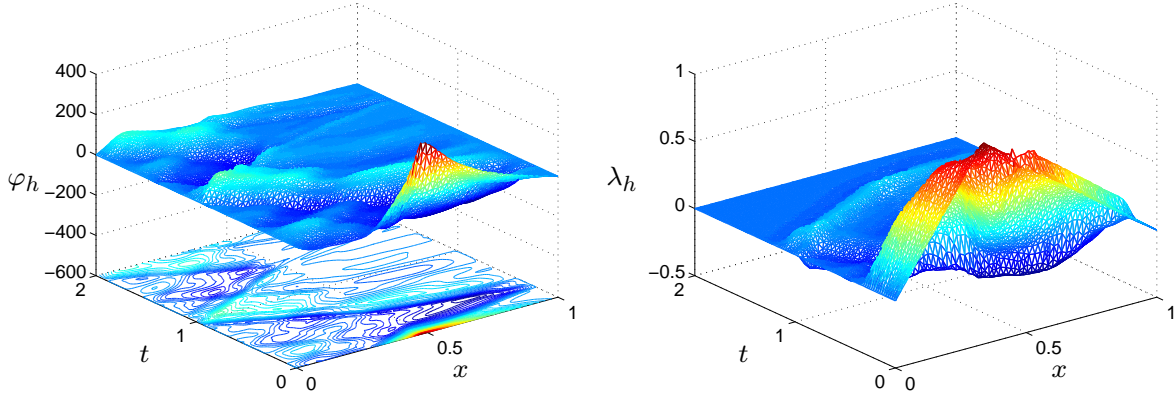


Figure 11: Example **EX3**, $\theta = 1/3$: $q_T = q_2^2$ for a non-constant velocity of propagation - Function φ_h (**Left**) and λ_h (**Right**) over Q_T .

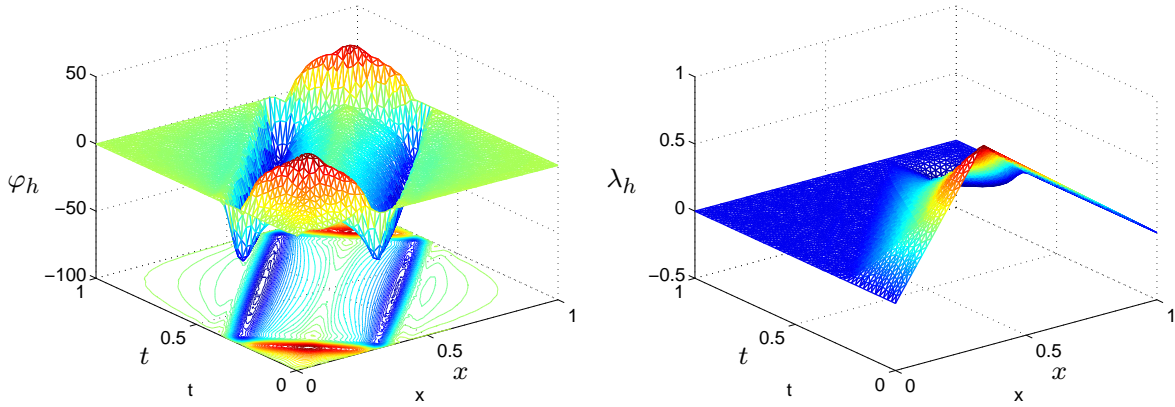


Figure 12: Example **EX3**, $\theta = 1/3$: $q_T = q_1^2$ - Function φ_h (**Left**) and λ_h (**Right**) over Q_T .

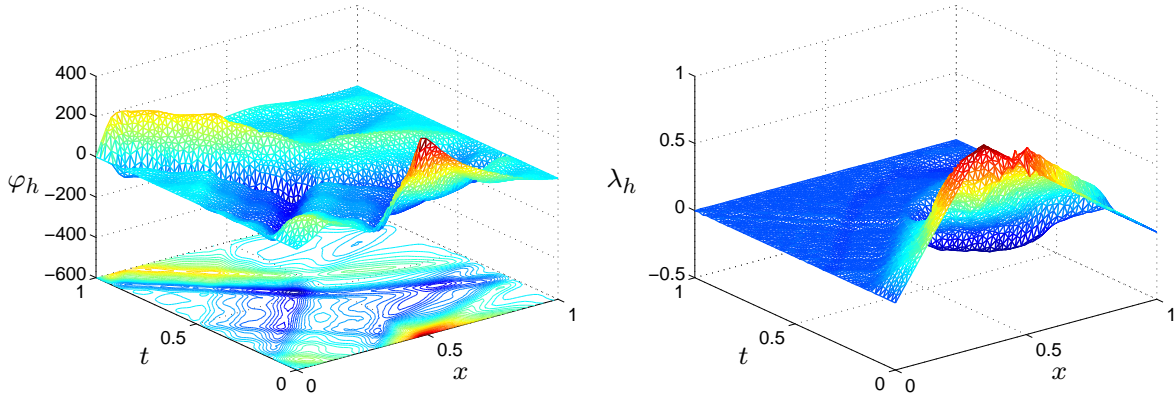


Figure 13: Example **EX3**, $\theta = 1/3$: $q_T = q_1^2$ for a non-constant velocity of propagation - Function φ_h (**Left**) and λ_h (**Right**) over Q_T .

4.10 Conjugate gradient for J^{**}

We illustrate here the Section 3.2: we minimize the functional $J^{**} : L^2(Q_T) \rightarrow \mathbb{R}$ with respect to the variable λ . We recall that this minimization corresponds exactly to the resolution of the mixed formulation (24) by an iterative Uzawa type procedure. The conjugate gradient algorithm is given

at the end of Section 3.2. In practice, each iteration amounts to solve a linear system involving the matrix $A_{r,h}$ of size $n_h = 4m_h$ (see (49)) which is sparse, symmetric and positive definite. We use the Cholesky method.

We consider the singular situation given by the example **EX3** with $\theta = 0.3$, $T = 2$ and $q_T = q_2^2$. We take $\varepsilon = 10^{-10}$ as a stopping threshold for the algorithm (that is the algorithm is stopped as soon as the norm of the residue g^n at the iterate n satisfies $\|g^n\|_{L^2(0,T;H_0^1(0,1))} \leq 10^{-10}\|g^0\|_{L^2(0,T;H_0^1(0,1))}$ or as the number of iterations is greater than 1000. The algorithm is initiated with $\lambda^0 = 0$ in Q_T . Table 10 and 11 display the results for $r = 10^{-1}$ and $r = 10^3$.

We first check that this iterative method gives exactly the same approximation λ_h than the previous direct method (where (49) is solved directly) since, from Proposition (3.1) problem (24) coincides with the minimization of J^{**} for $r > 0$. Then, we observe that the number of iterates is sub-linear with respect to the dimension $m_h = \text{card}(\{\lambda_h\})$ of the approximated problem. Once again, this is in contrast with the behavior of the conjugate gradient algorithm when this latter is used to minimize J^* with respect to (φ_0, φ_1) (see [22]).

Figure 14 displays the evolution of the residue $\|g^n\|_{L^2(0,T;H_0^1(0,1))}/\|g^0\|_{L^2(0,T;H_0^1(0,1))}$ with respect to the iteration n for two values of the augmentation parameter : $r = 10^{-1}$ and $r = 10^3$. The computation has been done with the level mesh $\sharp 3$. As expected, we check that a larger value of r improves significantly the convergence of the algorithm: recall that the gradient of J^{**} in $L^2(H^1)$ is given by: $\nabla J^{**}(\lambda) = A_r \lambda - \Delta^{-1}(L\varphi_0) := -\Delta^{-1}(L\varphi)$ and that r acts on the term $\|L\varphi\|_{L^2(H^{-1})}$. For a fixe level of mesh, we observe however a lower error $\|\lambda_h - y\|_{L^2(Q_T)}$ for $r = 10^{-1}$.

\sharp Mesh	1	2	3	4	5
h	7.18×10^{-2}	3.59×10^{-2}	1.79×10^{-2}	8.97×10^{-3}	4.49×10^{-3}
\sharp iterate	307	414	624	967	1000
$\ \lambda_h - y\ _{L^2(Q_T)}$	1.28×10^{-2}	4.77×10^{-3}	1.5×10^{-3}	6.2×10^{-4}	3.52×10^{-6}

Table 10: Conjugate gradient algorithm. **EX3** with $\theta = 1/3$, for control domain q_2^2 and $r = 10^{-1}$.

\sharp Mesh	1	2	3	4	5
h	7.18×10^{-2}	3.59×10^{-2}	1.79×10^{-2}	8.97×10^{-3}	4.49×10^{-3}
\sharp iterate	87	105	119	140	166
$\ \lambda_h - y\ _{L^2(Q_T)}$	1.15×10^{-1}	5.2×10^{-2}	1.65×10^{-2}	6.03×10^{-3}	2.89×10^{-3}

Table 11: Conjugate gradient algorithm. **EX3** with $\theta = 1/3$, for control domain q_2^2 and $r = 10^3$.

5 Concluding remarks and perspectives

We have extended in this work the contribution [10] to a non-cylindrical situation where the support of the controls depend on the time variable. The numerical approximation is based on a direct resolution of the controllability problem through a mixed formulation involving the dual adjoint variable and a Lagrange multiplier, which turns out to coincide with the primal state of the wave equation to be controlled. The well-posedness of this mixed formulation is the consequence of a generalized observability inequality deduced from [6] (and equivalent to the controllability of the equation). The approach leads to a variational formulation over time-space functional Hilbert space without distinction between the time and the space variable and is very appropriate to non-cylindrical situations.

At the practical level, the discrete mixed time-space formulation is solved in a systematic way in the framework of the finite element theory: in contrast to the classical approach, there is no need

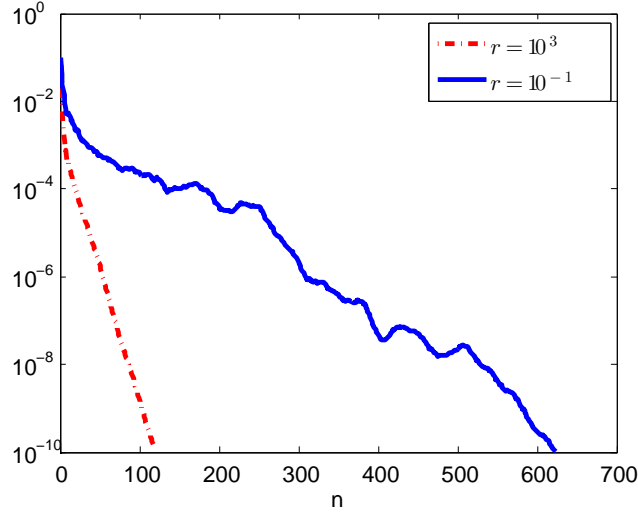


Figure 14: Example **EX3**. Evolution of the residue $\|g^n\|_{L^2(0,T;H_0^1(0,1))}/\|g^0\|_{L^2(0,T;H_0^1(0,1))}$ w.r.t. the iterate n .

to take care of the time discretization nor of the stability of the resulting scheme, which is often a delicate issue. The resolution amounts to solve a sparse symmetric linear system. As discussed in [10], Section 4.3 (but not employed here), the space-time discretization of the domain allows an adaptation of the mesh so as to reduce the computational cost and capture the main features of the solution.

The numerical experiments reported in this work suggest a very good behavior of the approach: the strong convergence of the sequences $\{v_h\}_{h>0}$, approximation of the controls of minimal square integrable norm, are clearly observed as the discretization parameter h tends to zero (as the consequence of the uniform inf-sup discrete property).

As briefly discussed in Section 4.7, this work opens now the possibility to optimize the control v of minimal $L^2(q_T)$ -norm with respect the support q_T (equivalently in our case, with respect to the curves a and b , see (6)) in the spirit of [23, 24, 25]: for any $(y_0, y_1) \in \mathbf{H}$, $T > 0$ and $L \in (0, 1)$, the problem reads :

$$\inf_{q_T \in C_L} \|v_{q_T}\|_{L^2(q_T)}, \quad C_L = \{q_T : q_T \subset Q_T, |q_T| = L|Q_T| \text{ and such that (11) holds}\}$$

where v_{q_T} denotes the control of minimal $L^2(q_T)$ norm for (1) distributed over q_T .

Eventually, we also mention that this approach which consists in solving directly the optimality conditions of a controllability problem may be employed to solve inverse problems where, for instance, the solution of the wave equation has to be recovered from a partial observation, typically localized on a sub-domain q_T of the working domain: actually, the optimality conditions associated to a least-square type functional can be expressed as a mixed formulation very closed to (24). These last two issues will be analyzed in a future work.

A Appendix: Fourier expansion of the control of minimal $L^2(q_T)$ -norm

We expand in this appendix in term of Fourier series the control of minimal $L^2(q_T)$ -norm v for (1) and the corresponding controlled solution y . We use these expansions in Section 4.6 to evaluate with respect to h , the error $\|y - \lambda_h\|_{L^2(Q_T)}$ and $\|v - v_h\|_{L^2(q_T)}$ where the sequence $(\varphi_h, \lambda_h)_{h>0}$

solves the discrete mixed formulation (39). We use the characterization of the couple (y, v) in term of the adjoint solution φ (see 5), unique minimizer in \mathbf{H} of J^* defined by (8).

We first note $(a_p, b_p)_{(p>0)}$ the Fourier coefficients in $l^2(\mathbb{N}) \times h^{-1}(\mathbb{N})$ of the minimizer $(\varphi_0, \varphi_1) \in L^2(0, 1) \times H^{-1}(0, 1)$ of (8), such that $(\varphi_0(x), \varphi_1(x)) = \sum_{p>0} (a_p, b_p) \sin(p\pi x)$. The adjoint state takes the form

$$\varphi(x, t) = \sum_{p>0} \left(a_p \cos(p\pi t) + \frac{b_p}{p\pi} \sin(p\pi t) \right) \sin(p\pi x).$$

We get

$$\begin{aligned} \iint_{q_T} |\varphi|^2 dx dt &= \sum_{p, q>0} a_p \overline{a_q} \iint_{q_T} \cos(p\pi t) \cos(q\pi t) \sin(p\pi x) \sin(q\pi x) dx dt \\ &+ \sum_{p, q>0} a_p \overline{b_q} \iint_{q_T} \cos(p\pi t) \frac{\sin(q\pi t)}{q\pi} \sin(p\pi x) \sin(q\pi x) dx dt \\ &+ \sum_{p, q>0} b_p \overline{a_q} \iint_{q_T} \frac{\sin(p\pi t)}{p\pi} \cos(q\pi t) \sin(p\pi x) \sin(q\pi x) dx dt \\ &+ \sum_{p, q>0} b_p \overline{b_q} \iint_{q_T} \frac{\sin(p\pi t)}{p\pi} \frac{\sin(q\pi t)}{q\pi} \sin(p\pi x) \sin(q\pi x) dx dt, \end{aligned} \quad (55)$$

and

$$\begin{cases} \int_0^1 \varphi_0(x) y_1(x) dx = \sum_{p>0} a_p \int_0^1 y_1(x) \sin(p\pi x) dx, \\ \langle \varphi_1, y_0 \rangle_{H^{-1}, H_0^1} = \sum_{p>0} b_p \int_0^1 y_0(x) \frac{\cos(p\pi x)}{p\pi} dx. \end{cases} \quad (56)$$

The optimality equation associated to the functional J^* (see 8) then reads

$$DJ^*(\varphi_0, \varphi_1) \cdot (\overline{\varphi_0}, \overline{\varphi_1}) = \iint_{q_T} \varphi \overline{\varphi} dx dt + \langle \overline{\varphi_1}, y_0 \rangle_{H^{-1}, H_0^1} - \int_0^1 \overline{\varphi_0} y_1 dx = 0, \quad \forall (\overline{\varphi_0}, \overline{\varphi_1}) \in \mathbf{H}$$

and can be rewritten in term of the $(a_p, b_p)_{p>0}$ as follows :

$$\left\langle \begin{pmatrix} \{\overline{a_p}\}_{p>0} \\ \{\overline{b_p}\}_{p>0} \end{pmatrix}, \mathcal{M}_{q_T} \begin{pmatrix} \{a_p\}_{p>0} \\ \{b_p\}_{p>0} \end{pmatrix} \right\rangle = \left\langle \begin{pmatrix} \{\overline{a_p}\}_{p>0} \\ \{\overline{b_p}\}_{p>0} \end{pmatrix}, \mathcal{F}_{y_0, y_1} \right\rangle \quad \forall (\overline{a_p}, \overline{b_p}) \in l^2(\mathbb{N}) \times h^{-1}(\mathbb{N}) \quad (57)$$

where \mathcal{M}_{q_T} denotes a symmetric positive definite matrix and \mathcal{F}_{y_0, y_1} a vector obtained from (55) and (56) respectively. The resolution of the infinite dimensional system (57) (reduced to a finite dimension one by truncation of the sums) allows an approximation of the minimizer (φ_0, φ_1) of J^* (see (8)), and then of φ , solution both of the boundary value problem (5) and of the mixed formulation (24).

Finally, we use that the corresponding control is given by $v = -\varphi 1_{q_T}$. We expand the corresponding controlled solution as $y(x, t) = \sum_{p>0} b_p(t) \sin(p\pi x)$ where, for all $p > 0$, the function b_p solves the ODE

$$\begin{cases} b_p''(t) + (p\pi)^2 b_p(t) = - \sum_{q>0} (a_q \cos(q\pi t) + b_q \sin(q\pi t)) c_{p,q}(t) := f_p(t), & t \in (0, T), \\ \sum_{p>0} b_p(0) \sin(p\pi x) = y_0(x), & \sum_{p>0} b_p'(0) \sin(p\pi x) = y_1(x) \end{cases}$$

with $c_{p,q}(t) := 2 \int_{a(t)}^{b(t)} \sin(p\pi x) \sin(q\pi x) dx$. The function b_p is given by

$$\begin{aligned} b_p(t) &:= C_{1p} \cos(p\pi t) + \frac{C_{2p}}{p\pi} \sin(p\pi t) \\ &+ \frac{1}{p\pi} \left(\sin(p\pi t) \int_0^t \cos(p\pi s) f_p(s) ds - \cos(p\pi t) \int_0^t \sin(p\pi s) f_p(s) ds \right) \end{aligned}$$

where $(C_{1p}, C_{2p})_{p>0}$ are the Fourier's coefficients of the initial data $(y_0, y_1) \in V$.

References

- [1] C. BARDOS, G. LEBEAU, AND J. RAUCH, *Sharp sufficient conditions for the observation, control, and stabilization of waves from the boundary*, SIAM J. Control Optim., 30 (1992), pp. 1024–1065.
- [2] M. BERNADOU AND K. HASSAN, *Basis functions for general Hsieh-Clough-Tocher triangles, complete or reduced*, Internat. J. Numer. Methods Engrg., 17 (1981), pp. 784–789.
- [3] P. B. BOCHEV AND M. D. GUNZBURGER, *Least-squares finite element methods*, vol. 166 of Applied Mathematical Sciences, Springer, New York, 2009.
- [4] J. H. BRAMBLE AND J. E. PASCIAK, *Least-squares methods for Stokes equations based on a discrete minus one inner product*, J. Comput. Appl. Math., 74 (1996), pp. 155–173. TICAM Symposium (Austin, TX, 1995).
- [5] F. BREZZI AND M. FORTIN, *Mixed and hybrid finite element methods*, vol. 15 of Springer Series in Computational Mathematics, Springer-Verlag, New York, 1991.
- [6] C. CASTRO, *Exact controllability of the 1-D wave equation from a moving interior point*, ESAIM Control Optim. Calc. Var., 19 (2013), pp. 301–316.
- [7] D. CHAPELLE AND K.-J. BATHE, *The inf-sup test*, Comput. & Structures, 47 (1993), pp. 537–545.
- [8] P. G. CIARLET, *The finite element method for elliptic problems*, vol. 40 of Classics in Applied Mathematics, Society for Industrial and Applied Mathematics (SIAM), Philadelphia, PA, 2002. Reprint of the 1978 original [North-Holland, Amsterdam; MR0520174 (58 #25001)].
- [9] N. CÎNDEA, E. FERNÁNDEZ-CARA, AND A. MÜNCH, *Numerical controllability of the wave equation through primal methods and carleman estimates*, ESAIM Control Optim. Calc. Var., 19 (2013), pp. 1076–1108.
- [10] N. CÎNDEA AND A. MÜNCH, *A mixed formulation for the direct approximation of the control of minimal L^2 -norm for linear type wave equations*, <http://hal.archives-ouvertes.fr/hal-00853767>.
- [11] L. CUI, X. LIU, AND H. GAO, *Exact controllability for a one-dimensional wave equation in non-cylindrical domains*, J. Math. Anal. Appl., 402 (2013), pp. 612–625.
- [12] J. W. DANIEL, *The approximate minimization of functionals*, Prentice-Hall Inc., Englewood Cliffs, N.J., 1971.
- [13] D. A. DUNAVANT, *High degree efficient symmetrical Gaussian quadrature rules for the triangle*, Internat. J. Numer. Methods Engrg., 21 (1985), pp. 1129–1148.
- [14] M. FORTIN AND R. GLOWINSKI, *Augmented Lagrangian methods*, vol. 15 of Studies in Mathematics and its Applications, North-Holland Publishing Co., Amsterdam, 1983. Applications to the numerical solution of boundary value problems, Translated from the French by B. Hunt and D. C. Spicer.
- [15] R. GLOWINSKI, *Handbook of numerical analysis. Vol. IX*, Handbook of Numerical Analysis, IX, North-Holland, Amsterdam, 2003. Numerical methods for fluids. Part 3.

- [16] R. GLOWINSKI AND J.-L. LIONS, *Exact and approximate controllability for distributed parameter systems*, in Acta numerica, 1995, Acta Numer., Cambridge Univ. Press, Cambridge, 1995, pp. 159–333.
- [17] R. GLOWINSKI, J.-L. LIONS, AND J. HE, *Exact and approximate controllability for distributed parameter systems*, vol. 117 of Encyclopedia of Mathematics and its Applications, Cambridge University Press, Cambridge, 2008. A numerical approach.
- [18] A. Y. KHAPALOV, *Controllability of the wave equation with moving point control*, Appl. Math. Optim., 31 (1995), pp. 155–175.
- [19] J.-L. LIONS, *Contrôlabilité exacte, perturbations et stabilisation de systèmes distribués. Tome 1*, vol. 8 of Recherches en Mathématiques Appliquées [Research in Applied Mathematics], Masson, Paris, 1988. Contrôlabilité exacte. [Exact controllability], With appendices by E. Zuazua, C. Bardos, G. Lebeau and J. Rauch.
- [20] P. MARTIN, L. ROSIER, AND P. ROUCHON, *Null controllability of the structurally damped wave equation with moving control*, SIAM J. Control Optim., 51 (2013), pp. 660–684.
- [21] A. MEYER, *A simplified calculation of reduced hct-basis functions in a finite element context*, Comput. Methods Appl. Math., 12 (2012), pp. 486–499.
- [22] A. MÜNCH, *A uniformly controllable and implicit scheme for the 1-D wave equation*, M2AN Math. Model. Numer. Anal., 39 (2005), pp. 377–418.
- [23] ———, *Optimal design of the support of the control for the 2-D wave equation: a numerical method*, Int. J. Numer. Anal. Model., 5 (2008), pp. 331–351.
- [24] A. MÜNCH AND F. PERIAGO, *Optimal distribution of the internal null control for the one-dimensional heat equation*, J. Differential Equations, 250 (2011), pp. 95–111.
- [25] F. PERIAGO, *Optimal shape and position of the support for the internal exact control of a string*, Systems Control Lett., 58 (2009), pp. 136–140.
- [26] P.-F. YAO, *On the observability inequalities for exact controllability of wave equations with variable coefficients*, SIAM J. Control Optim., 37 (1999), pp. 1568–1599.